

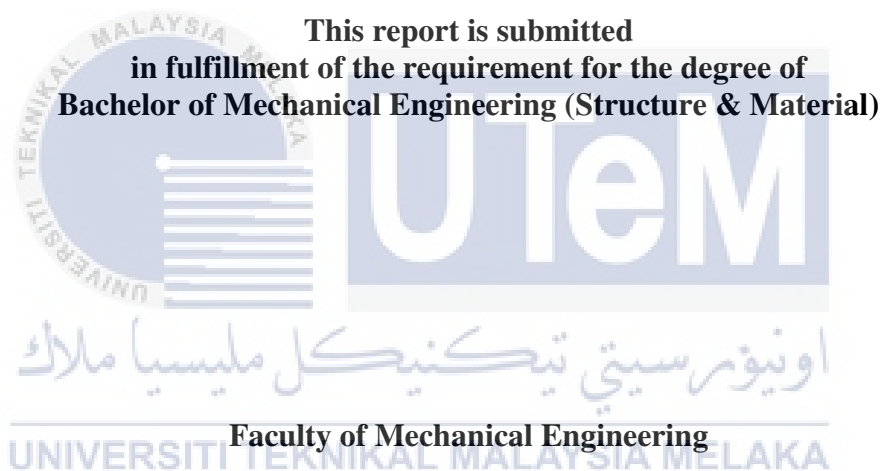
**FINITE ELEMENT ANALYSIS OF LOCALLY MANUFACTURED ENGINE MOUNTING
COMPONENTS UNDER CYCLIC STRESSES AND THERMAL LOADING**



UNIVERSITI TEKNIKAL MALAYSIA MELAKA

**FINITE ELEMENT ANALYSIS OF LOCALLY MANUFACTURED ENGINE
MOUNTING COMPONENTS UNDER CYCLIC STRESSES AND THERMAL
LOADING**

AZMEIRUL AZRIE BIN MOHD SHAH



UNIVERSITI TEKNIKAL MALAYSIA MELAKA

JUNE 2017

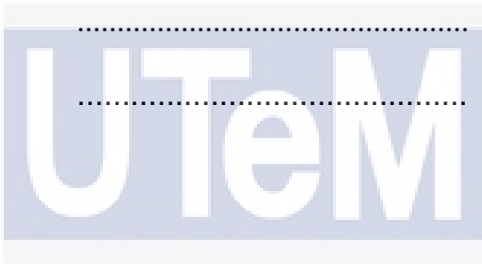
DECLARATION

I declare that this project report entitled “Finite Element Analysis of Locally Manufactured Engine Mounting Components Under Cyclic Stresses and Thermal Loading” is the result of my own work except as cited in the references

Signature :

Name :

Date :



اونيورسيتي تيكنيكل مليسيا ملاك
UNIVERSITI TEKNIKAL MALAYSIA MELAKA

APPROVAL

I hereby declare that I have read this project report and in my opinion this report is sufficient in terms of scope and quality for the award of the degree of Bachelor of Mechanical Engineering (Structure & Materials).

	Signature :
	Name of Supervisor :
	Date :

اونيورسيتي تيكنيكل مليسيا ملاك
UNIVERSITI TEKNIKAL MALAYSIA MELAKA

DEDICATION

Dedicated to my beloved mother and father who always encouraged and supported me.



ABSTRACT

The main purpose of an engine mounting components is to support the powertrain system in an automobile which subject to thermal loading. This study examines a methodology to predict the fatigue life of an engine mounting component using ANSYS software. An engine mounting component is modeled using CATIA software and FE analysis is carried out using ANSYS software. The critical condition caused by the cyclic load and thermal loading may lead to component failure. The scope of the study is to analyze the design, optimize and compare between the two types of engine mounting component under cyclic stresses and thermal loading. The stress concentration factors were estimated based on the structural analysis. The structural analysis is performed on specified part for a given load and support conditions. In order to use a finite element analysis it is necessary to know the mechanical properties of the material. The tensile test, Rockwell hardness test and thermal inspection were conducted in this study to determine the mechanical properties and thermal behavior of an engine mounting component. The simulation of fatigue analysis by finite element software on the existing PROTON SAGA and PERODUA KANCIL engine mounting component to determine the maximum stress and fatigue life on the model due to the effect of thermal loading and cyclic stresses. The final simulation results obtained in this study shows that the higher thermal loading will cause a lower fatigue resistance or shorter life of an engine mounting component.

ABSTRAK

Tujuan utama komponen mounting enjin adalah untuk menyokong sistem rantai kuasa dalam sesebuah kenderaan tertakluk kepada beban suhu. Kajian ini mengkaji tentang kaedah untuk meramalkan jangka hayat kelesuan komponen mounting enjin dengan menggunakan perisian ANSYS. Komponen mounting enjin dimodelkan menggunakan perisian CATIA dan kajian analisis unsur terhingga menggunakan perisian ANSYS. Keadaan kritikal disebabkan oleh beban tekanan dan beban haba yang menjadi punca kepada kegagalan komponen tersebut. Skop kajian ini adalah untuk menganalisis reka bentuk dengan mengoptimumkan dan membuat perbandingan antara dua pengeluar komponen mounting enjin dibawah beban kitaran tekanan dan beban haba. Faktor penumpuan tegasan telah dianggarkan berdasarkan analisis struktur. Analisis struktur dilakukan pada bahagian tertentu dalam keadaan tekanan dan sokongan. Untuk menggunakan analisis unsur terhingga adalah perlu mengetahui ciri-ciri mekanikal pada bahan komponen tersebut. Ujian tegangan, ujian kekerasan Rockwell dan pemeriksaan haba telah dijalankan dalam kajian ini untuk menentukan ciri-ciri mekanikal dan sifat pada komponen mounting enjin. Simulasi analisis jangka hayat kelesuan pada model PROTON SAGA dan PERODUA KANCIL pada komponen mounting enjin untuk menentukan tegasan maksimum dan jangka hayat kelesuan kesan terhadap beban haba dan beban tekanan. Keputusan akhir simulasi yang diperolehi melalui kajian ini menunjukkan bahawa semakin tinggi beban suhu dikenakan akan menyebabkan ringtangan kelesuan menjadi lebih rendah atau jangka hayat yang lebih pendek pada komponen mounting enjin tersebut.

ACKNOWLEDGEMENT

First and foremost, I would like to take this opportunity to express my sincere thanks to my supervisor Profesor Madya Abd. Salam Bin Md. Tahir from the Faculty of Mechanical Engineering Universiti Teknikal Malaysia Melaka (UTeM) for his valuable contribution on advising and supervising this dissertation. He never hesitated to give me advice and guidance whenever I confronted problems. I am thankful for his patience and advice while guiding me in doing this dissertation.

Secondly, I would like to express my appreciation to FKM's assistant engineers; En. Wan Saharizal Bin Wan Harun (Tensile Test), En. Mohd Hairi Bin Md. Rahim (Lathe Machine), En. Mahader Bin Muhamad (Hardness Test), En. Mad Nasir Bin Ngadiman (Automotive Workshop) and En. Asjufry Bin Muhajir (Thermal Imaging Camera) for their valuable time and assistance in offering their suggestions or ideas and provided me the equipment and devices to obtain the useful data which helps in strengthening the content of this dissertation.

Finally, thanks to all who were involved in this dissertation directly or indirectly especially my family in order to complete this project successfully.

TABLE OF CONTENTS

CHAPTER	CONTENT	PAGE
	SUPERVISOR'S DECLARATION	iii
	TABLE OF CONTENT	viii
	LIST OF FIGURES	xii
	LIST OF TABLE	xv
	LIST OF ABBREVIATIONS	xvi
	LIST OF SYMBOLS	xvii
CHAPTER 1	INTRODUCTION	1
	1.1 Background of Project	1
	1.2 Problem Statement	3
	1.3 Objective	4
	1.4 Scope of Project	4
CHAPTER 2	LITERATURE REVIEW	5
	2.1 Introduction	5
	2.2 Type of Engine Mount Component	5
	2.2.1 Passive Hydraulic Mounts	6
	2.2.2 Active Mounts	6
	2.2.3 Elastomeric Mounts	7
	2.3 Engine Mounting System	8
	2.3.1 Modeling Engine Mount	8
	2.3.2 Engine Mounting Characteristic	9
	2.4 Mechanical Testing	10
	2.4.1 Tensile Testing	10
	2.4.2 Hardness Testing	11
	2.5 Fatigue Failure Analysis	12
	2.5.1 Experimental	13
	2.5.2 Static Structural Analysis Model	14

2.6	Fatigue Failure under Cyclic Stress	14
2.6.1	S-N Curve	16
2.6.2	Goodman Diagram	17
2.7	Material	18
2.7.1	AISI/SAE 4130	18
2.7.2	Elastomer (Butyl Rubber)	19
2.8	Manufacturing Process	19
2.8.1	Rubber to Metal Bonding Process	20
2.8.2	Welding Process	21
2.9	Finite Element Analysis	21
2.9.1	ANSYS Software	22
2.9.2	Modeling on Finite Element Analysis	22
2.9.2.1	1D Element Modelling	22
2.9.2.2	2D Element Modelling	23
2.9.2.3	3D Element Modelling	23
CHAPTER 3	METHODOLOGY	25
3.1	Introduction	26
3.2	Project Flow Chart	25
3.3	Development of Experiment	27
3.4	Tensile Test	27
3.4.1	Theory	27
3.4.2	Test Specimen	27
3.4.3	Procedure	28
3.4.4	Formula	28
3.4.5	The Results of Tensile Test	30
3.4.6	Material Properties	32
3.5	Hardness Testing	33
3.5.1	Theory	33
3.5.2	Test Specimen	34
3.5.3	Procedure	34
3.5.4	Hardness Results	35
3.6	Thermography Inspection	36

3.6.1	Thermography Result	36
3.7	Generation of CAD Model	38
3.8	Static Structural Analysis	39
3.8.1	Material Properties	39
3.8.2	Mesh Generation	42
3.8.3	Load Condition	43
3.8.4	Boundary Condition	44
3.8.5	Thermal Loading Condition	44
CHAPTER 4	RESULT AND DISCUSSION	46
4.1	Introduction	46
4.2	Mechanical Testing Experimental Work	46
4.3	A static Structural Analysis	47
4.3.1	The Von Misses Stress Analysis on the Elastomer with Thermal Effect	49
4.3.2	Total Deformation and Safety of Factor with Thermal Loading Effect on the Elastomer	53
4.3.3	Fatigue Analysis with Thermal Loading Effect of Steel Part	55
CHAPTER 5	CONCLUSION AND RECOMMENDATION	62
5.1	Conclusion	62
5.2	Recommendation	63
	REFERENCE	64
	APPENDICES	67
A	ASTM E-08 Metallic Tensile Test Standard	68
B	Technical Drawing – Specimen for Tensile Test	69
C	Result of Tensile Test Specimen	70
D	Sample Calculation for Tensile Test	73
E	Hardness Conversion Table	74
F	Technical Drawing – Proton SAGA Engine Mounting	75

G	Technical Drawing – Perodua KANCIL Engine Mounting	76
H	Gantt Chart of PSM I and PSM II	77



LIST OF FIGURES

FIGURE	TITLE	PAGE
1.1	The Schematic Diagram of Engine Mounting Component	1
1.2	Location of Engine Mounting Component	2
1.3	Engine Mount Bracket Analysis	3
2.1	Schematic Diagram of Passive Hydraulic Mounts	6
2.2	Schematic Diagram of An Active Engine Mount	7
2.3	Elastomeric Mounts Component	7
2.4	The Six Degree of Freedom (DOF) Force Excitation	8
2.5	An Engine Mounting System	9
2.6	The Stress-Strain Curve of The Ductile Material	11
2.7	Experimental Test Conduct in Longitudinal and Transversal Direction	13
2.8	Flow Chart for Static Structural Analysis	14
2.9	Constant Amplitude Loading	15
2.10	S-N Curve for Fatigue Life Evaluation	16
2.11	Goodman Diagram	17
2.12	The Specification of Engine Mount Component	20
2.13	Two Dimension (2D) Element Modeling	23
2.14	Three Dimension (3D) Element Structures	24
3.1	Project Flow Chart for Project	26

3.2	Round Tension Test Specimen	28
3.3	Gauge Length at Failure of Specimen 1	30
3.4	Result Tensile Test of Three Specimen	31
3.5	The Appearance Cup and Cone Fracture in a Ductile Metal	32
3.6	Rockwell Hardness Tester Indenter	33
3.7	Setup of Hardness Test	35
3.8	The Thermal Imaging Inspection on the Component	37
3.9	Isometric View (3D) model of PROTON SAGA Component	38
3.10	Isometric View (3D) model of PERODUA KANCIL Component	39
3.11	Flow Chart of the Structural Analysis Method	39
3.12	S-N curve displayed and interpolated as Linear	41
3.13	Meshed Model of Engine Mounting Component	42
3.14	Mesh Quality Metrics Bar Graph	43
3.15	The direction of Force Applied on Component	43
3.16	Fixed Constraints	44
3.17	The Thermal Loading on the Component	45
4.1	The Three Dimensional Model of the Proton SAGA Component	48
4.2	Maximum Stress of Elastomer Mount at Different Temperature	50
4.3	Graph of Von Misses Stresses with Thermal Loading	51
4.4	The Maximum Stress Region on the Proton SAGA Component	52
4.5	The Maximum Stress Region on the Perodua KANCIL Component	52
4.6	The Maximum Total Deformation of Elastomer Mount	53

4.7	The Factor Safety of Elastomer Mount	54
4.8	S-N Curve Displayed and Interpolated as log-log	56
4.9	Contour Plot of Equivalent Alternating Stress over the Rod	58
4.10	Graph of Fatigue Equivalent Alternating Stress with Thermal Loading	60
4.11	The Fatigue Life of Elastomer Mount Perodua KANCIL	60
4.12	The Fatigue Life of Elastomer Mount Proton SAGA	61



LIST OF TABLES

TABLES	TITLE	PAGE
3.1	Detailed Tensile Test Specimen Dimensions	30
3.2	Experimental Data of Tensile Test for Three Specimen	32
3.3	Rockwell Hardness Scales	35
3.4	Results of Hardness Test	36
3.5	Temperature Data of Engine Mounting Component	37
3.6	Properties of AISI/SAE 4130 Steel	40
3.7	Properties of Elastomer	40
3.8	Properties of Alternating Stress Mean Stress	41
4.1	Summary of Mechanical Properties of an Engine Mounting Component Material	46
4.2	Mechanical Properties of Experimental AISI 4130 Steel	47
4.3	The Engineering Data for Simulation in ANSYS Workbench	48
4.4	The Results Von Mises Stress with Thermal Loading	50
4.5	The Specification of the Elastomer Part	53
4.6	Properties of Fatigue Modification	55
4.7	S-N Curve Displayed and Interpolated As Linear	58
4.8	The Results Equivalent Alternating Stress with Thermal Loading	59
4.9	The Size of Connecting Rod	59

LIST OF ABBREVIATIONS

FEA	Finite Element Analysis
CAD	Computer Aided Design
CATIA	Computer Aided Three Dimensional Interactive Application
ANSYS	American Computer-Aided Engineering Software
FEM	Finite Element Model
PROTON	Perusahaan Otomobil Nasional
PERODUA	Perusahaan Otomobil Kedua Sendirian Berhad
NVH	Noise and Vibration Harshness
DOF	Degree of Freedom
ASTM	American Society for Testing and Materials
AISI	American Iron and Steel Institute
SAE	Society of Automotive Engineer
S-N	Stress versus Fatigue Life (N) Relation or Curve
MIG	Metal Inert Gas
TIG	Tungsten Inert Gas
SOF	Safety of Factor

LIST OF SYMBOL

M	=	Mass
K	=	Stiffness
C	=	Damping
σ_a	=	Stress Amplitude
σ_u	=	Ultimate Stress @ Tensile strength
σ_m	=	Mean Stress
σ_f	=	Fracture Strength
σ_w	=	Allowable Stress or Working stress
σ_n	=	Stress at zero mean stress
S_e	=	Stress Endurance Limit or Fatigue Limit
N_f	=	Number of Cycles to Failure
E	=	Young's Modulus
ν	=	Poisson's Ratio
ρ	=	Density
ξ	=	Damping Ratio
F_e	=	Excitation Force
l_o	=	Original Length
ε	=	Strain
P_y	=	Load at Yielding
A_o	=	Original Cross-Sectional Area
A_o	=	Operating Frequency

CHAPTER 1

INTRODUCTION

1.1 Background of Project

Engine mounting components are used to grip the main support structure (chassis) across the automotive engine. Figure 1.1 shows the schematic diagram of locally assemble of an engine mounting component system. Basically, engine mounting components are usually made up by metallic and rubber materials. The metal parts are used as the frame of mounting that connects the engine and structure of car's body. The rubber part acting as a stiffener to provide flexibility on the vehicle's engine. If an engine mounting component does not have any appropriate level of stiffness it can cause high noise and vibration. An automotive engine is one of the source of vibrations of the car or vehicle. These vibrations are induced by forces transmitted by the engine mount elements onto the structure frame. Therefore it is very important that an engine mounting components have enough stiffness as well as strength.

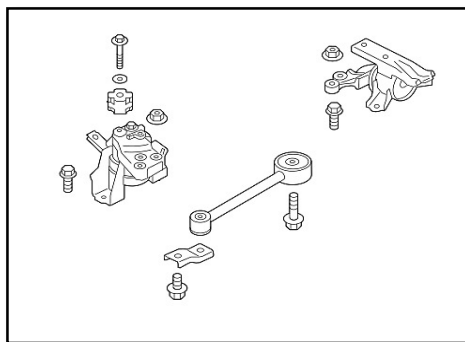


Figure 1.1: The Schematic Diagram of Engine Mounting Component

Source: (Heisler, 2002)

The primary function of an engine mounting is to transmit the vibration. It is filled with rubber to reduce the engine vibration and ensure that there is no direct contact between metal to metal surfaces and between the engine and the structure of the car body. It is the most critically loaded component and experiences a high cyclic loads with thermal loading during its service life. Usually, engine mounts function in very a harsh environment at a low and high temperatures combining with aggressive substances such as oil, gasoline and cleaning liquid (S.H. Lee, Y.S Lim, 2006).

An engine mounting components need to go through analysis to verify the engine mount properties in the design stage (A.Agharkakli,D. P. Wagh, 2013). The cyclic stresses and thermal loading are applied with the boundary conditions during analysis. This study focuses on two type of an engine mounting component for the locally manufactured passenger's car. Figure 1.2 shows an engine mounting component of the Proton SAGA that was used in this study.



Figure 1.2: Location of Engine Mounting Component

The Finite Element Analysis (FEA) has been developed for the last twenty years as a powerful tool in various fields of product development and research. Thus, in this study FEA will be employed as the tool to carry out stress-strain analysis on the chosen engine mounting component. Figure 1.3 (Maski & Basavaraj, 2015) shows the example of analysis with meshing using FEA on engine mounting bracket. The results are correlated with the mechanical properties and the conclusions are drawn accordingly.

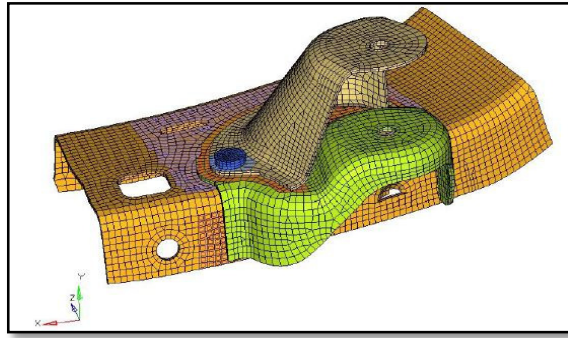


Figure 1.3: Engine Mount Bracket Analysis

Source: (Maski & Basavaraj, 2015)

1.2 Problem Statement

An automotive engine mounting component is the most important part that holds the engine to the structure or body on vehicle system. It also provides insulation to the vibration generated from the vehicle's engine to the chassis. Besides that, it holds the engine at certain position that allowing minimum movement, noise and vibration of the vehicle.

The most common problem of existing engine mounting rod is when its rubber part breaks down due to rapidly increase vibrations of the engine at different speed and various thermal load conditions. The rubber part will eventually degrade and fail over time due to high cycles of loading. A failure of an engine mount can cause an increase in engine noises and vibration. An engine mounting components has been designed to have a specific life-span. It needs to be replaced after a few thousand cycles of loading or when the noise level around the engine compartment becomes very high than its normal level. Thus there is a need to predict the life-span of the component before it causes severe damage to the vehicle.

In this project, the FEA of an engine mounting component is studied and analyzed by focusing on the effects of cyclic stresses and thermal loading for the existing two generation of segment C passenger cars. Lastly, a systematic study is required to undertake a detailed investigation in order to understand the dynamic behavior and structural characteristics of the components.

1.3 Objective

The main objective of this project is to perform FEA on the locally manufactured engine mounting component subjected to cyclic stresses and thermal loading.

1.4 Scope of Project

The computational analysis based on the FEA will be carried out on the selected design of engine mounting components. Two types of brand that were manufactured for C-Segment of passenger cars for the engine mounting component with all constant dimensions will be chosen and analyzed. The two brands of locally manufactured component chosen for the analysis are used for PROTON SAGA and PERODUA KANCIL passenger car. The scope of this project is outlined below;

1. To generate Computer Aided Design (CAD) model of engine mounting component by using the Computer Aided Three Dimensional Interactive Application (CATIA) software.
2. To perform FEA by using the CAD model of engine mounting components under the cyclic stresses and thermal loading using ANSYS software.
3. To analyze the design, optimize and compare between the two brands locally manufactured of an engine mounting component under cyclic stresses and thermal loading.
4. The stress concentration factors will be estimated based on results of FEA. The results of FEA will help to make component's refinement and optimization and also to propose improvement about its life-span.

CHAPTER 2

LITERATURE REVIEW

2.1 Introduction

This chapter discuss the literature study which related to locally manufacture an engine mounting component under cyclic stress and thermal loading using finite element analysis (FEA).

2.2 Type of Engine Mount Component

Basically, an engine vehicle mounting system usually consists of an engine and several mounts connected to the vehicle structure. Then, a modern engine mounting system have been used successfully to isolate the driver and passenger from noise and vibration generated by the engine when travelling in the vehicles. The noise characteristics of a vehicle are significantly affected by vibration transferred to the car body through the chassis mounting points from the engine and suspension (Michael Champrenault, 2007) . Generally, the main function of engine mount is to reduce the dynamic force and vibration. The mounting system will provide isolation that will minimize the transmitted forces from the structure body. An engine mount are expected to function in a very harsh environment such as at a very low and high temperatures combined with aggressive substances such as oil, gasoline and cleaning liquid. After that, (Yu, Naganathan, & Dukkupati, 2001) state that the entire engine mounting system is not only depends on the performance of individual mounts, but the optimum design of the whole system. However, there are different kinds of an engine mounting system that can increase the performance of power train system such as passive hydraulic mounts, active mounts and elastomeric mounts. Three different types of engine mount systems are described in the proceeding sections.

2.2.1 Passive Hydraulic Mounts

The automotive industry is widely used this type of mount because it reduces more engine vibration and noise. Moreover, (Kim, 1992) claims that the hydraulic mounts are first introduced in 1962 for use as vehicle mounting systems. The suitable function for this type of mounts for vehicles tends to be small, lightweight and front wheel drive with low idle speeds. A general schematic diagram of the hydraulic mount is shown in Figure 2.1. This mount can be tuned to have high damping at the shock excitation frequency which is used to reduce the vibration levels. Lastly, the dynamic stiffness of these mounts is usually higher than the elastomeric mounts (Y. Naganathan, 2001).

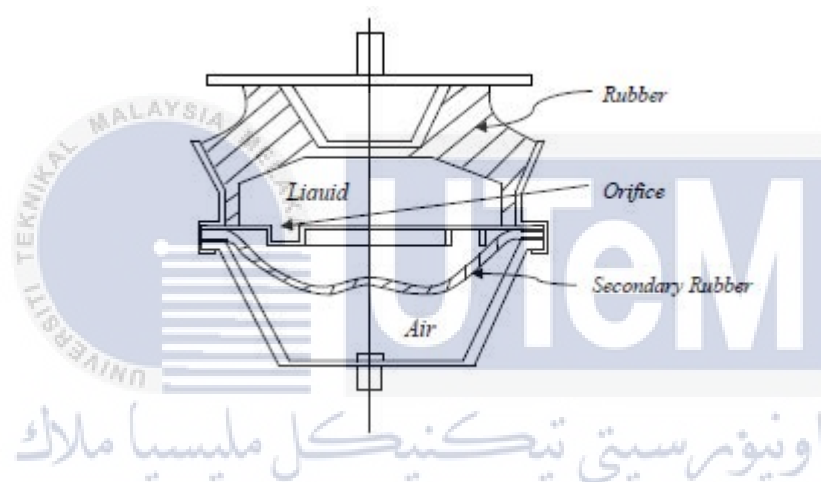


Figure 2.1: Schematic Diagram of Passive Hydraulic Mounts

Source: (J.C.Snowdon, 1968)

2.2.2 Active Mounts

Generally, active engine mount consists of passive mount and elastomer or hydraulic. It provides an effective solution to further improve the acoustic and vibrational comfort of passenger car (Hausberg, 2015). The system can be very stiff at low frequencies because the active mounts use sensors, control unit and an energy source. However, a typical active engine mounts and its control system is shown in Figure 2.2 (Jansson & Johansson, 2003) where it contains fluid as a medium of damping.

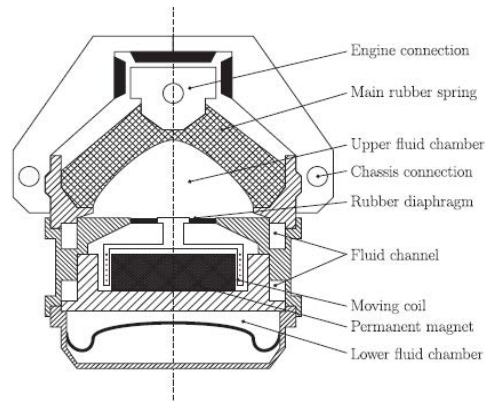


Figure 2.2: Schematic Diagram of an Active Engine Mount

Source: (Jansson & Johansson, 2003)

2.2.3 Elastomeric Mounts

The elastomeric or rubber mounts have been used to isolate vehicle structure from engine vibration since the 1930s in automotive industry. The current trends and future prospect of mobility industry focus more on better performance of the elastomeric mounts (Miller, 1992). This mount is extensively used in many applications because of their large reversible elastic deformation, excellent damping and energy absorption characteristics. Moreover, rubber mount act as primary vibration because it could not meet more stringent requirement especially for the non-linear excitation situation (Zhang Yunxia, 2008). In facts, the rubber mounts has been designed for necessary elastic stiffness rate characteristics in all directions for proper vibration isolation. This type of engine mount offer economic advantages because the type of mount is compact, cost-effective and maintenance free. A simple elastomeric mount is shown in Figure 2.3 widely used in automotive application.



Figure 2.3: Elastomeric Mounts Component

2.3 Engine Mounting System

The primary function of an engine mount is attaching or linking between the engines or transmission unit to the chassis body of the car. An engine mounting system generally consists of an engine that is vibration source and several mounts connected to the chassis of vehicle structure. Then, (S.Koushik, 2013) state that the effects of the noise and vibration harshness (NVH) characteristic of engine mounts are unlimited due to the nature of the use of the machine. It is an important part of the automotive system to reduce the vibration and noise of the vehicle. Besides that, it also supports the engine weight and the major function of engine mounts is to isolate the unbalance engine disturbance force from the vehicle structure. Based on the six degree of freedom (DOF) engine model, the system disturbances will excite the engine in various vibration modes as shown in Figure. 2.4.

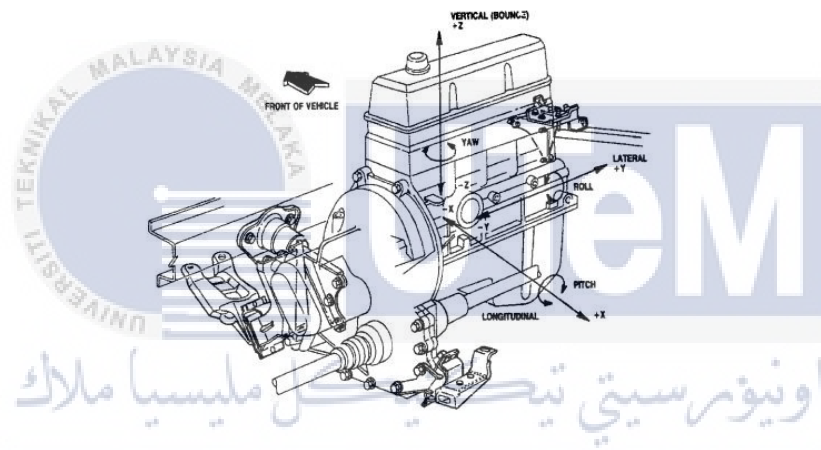


Figure 2.4: The Six Degree of Freedom (DOF) Force Excitation

Source: (P.E Geck, 1992)

2.3.1 Modeling Engine Mount

There are two type of forces disturbance generated to the structural (chassis) of the vehicle. The force disturbance created from the road condition like bumps, pot holes and geometry. Then, the force is transmitted from the engine to the chassis that can also generate force disturbance (Darsivan, F Jashi, Martono, 2006). Basically, the engine mounting system can be presented by spring, mass and damper as shown in Figure 2.5 for the single mounts. The mass represents as the engine of the vehicle, spring and damper represent the engine mount and the ground represents the structural chassis of the vehicle.

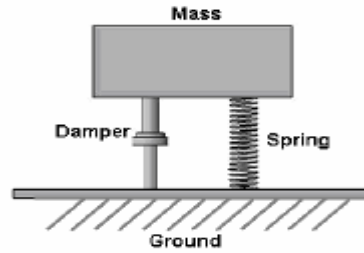


Figure 2.5: An Engine Mounting System

Source: (Darsivan, F Jashi, Martono, 2006)

2.3.2 Engine Mounting Characteristic

A typical engine mounting system includes an engine, engine mounts and a foundation. The engine is free to oscillate on its mounts depending on the direction of excitations (Hagino, 1991). In static structural analysis, it needs a rigid element as a boundary condition. A static analysis deals with the conditions of the equilibrium of the bodies acted by forces. So, the engine mounting component holes act as a rigid element which has its degree of freedom fixed. The element which is used to fix component and structure body of vehicle is fixed by constraining six DOF.

The equation of motion for a six DOF engine model with N mounts and rigid foundation is given by equation (2.1):

$$[M]\{\ddot{X}\} + [C]\{\dot{X}\} + [K]\{X\} = \{F\} \quad (2.1)$$

where X, \dot{X}, \ddot{X} are the 6 x 1 displacement, velocity and acceleration vectors at the centre of gravity of the engine, $[M]$ the 6 x 6 engine rigid mass matrix, $[K]$ the 6 x 6 system complex stiffness matrix, and $[C]$ is the 6x6 viscous damping matrix. The force $\{F\}$ represents a 6 x 1 vector of excitation forces and moments. This equation about the dynamic response and the function of the system that can be easily derived. Furthermore, in real condition of vehicle system there are many kinds of vibration modes in the foundation. Therefore, (J.Bretl, 1993) claimed that there are many research works on engine mounting component based on the kinds of vibration modes.

2.4 Mechanical Testing

In this project the mechanical testing are carried out to determine the properties or behavior of an engine mounting component. Most recently (M.S. Loveday, 1998) described that a mechanical test can be used to determine the properties of the material such as tensile or ultimate strength, percentage of elongation, Young's modulus, yield strength and hardness. However, the mechanical testing are usually related to defining the elastic and plastic behavior of the material (Gliner, 1960). Hence, there are several types of test can be used to determine various physical and mechanical properties of material. The development of experiment technique was carried out to classify and identify the properties of the material that can be used in simulation analysis as engineering data. The mechanical testing that are particularly relevant in this project are tensile and hardness tests. The American Society for Testing and Materials (ASTM) physical and mechanical testing standards are used as a guide for the proper procedure, design and dimension of the specimen and calculation of results for the tests.

2.4.1 Tensile Test

Tensile test is a method of subjecting a test specimen to uniaxial load under quasi-static condition until it fails. In this test a specimen of standardized dimension is subjected to an axial load at a specific extension rate until failure or fracture of the specimen. Then, the tensile test is probably the most fundamental type of mechanical test because the test are simple, relatively inexpensive and fully standardized (Bobbili, 2015). Moreover, the tensile test will produce stress-strain curve when an increasing tensile load or stress is applied on the material until it breaks. A stress-strain curve obtained from this tensile test will be used to determine the result of mechanical behaviour or properties of the ductile material as shown in Figure 2.6. From the stress-strain curve, properties such as the elastic deformation limit (yield point), plastic deformation, yield and ultimate strengths and Young's modulus of the material can be obtained. In this project, a standard specimen is prepared in a round shape by following the ASTM-E8 standard, which is a standard test method for tension testing of metallic materials. Lastly, those mechanical properties are important to be known since it will be used in a fatigue analysis that will describe the material responds to cyclic loading.

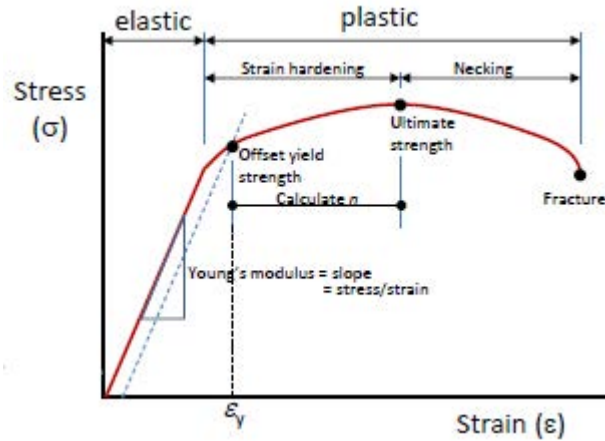


Figure 2.6: The Stress-Strain Curve of The Ductile Material

Source: (Philipfigari, 2008)

2.4.2 Hardness Test

Generally, the hardness is one of the most basic mechanical properties of an engineering material. The hardness test is defined as the resistance to indentation in order to measure the permanent depth of the indentation. The hardness value of the material is obtained by measuring the area of the indentation on the surface of test's specimen (Meyer, 1989). The test is fast, inexpensive and relatively non-destructive by leaving only small indentation on the test specimen. Moreover, the result is a lower hardness if a deeper or wider indentation indicates on the specimen that also means a less resistance of the material. In this project, the Rockwell hardness will be used to determine the hardness of the specimen engine mounting component. The standard test method according to the American Society Testing and Material (ASTM) is followed which is ASTM E18 for Rockwell hardness of metallic material. After that, the testing procedure by indenting a flatly ground metal surface with a diamond indenter. A minor load H_1 as the depth of the impression will be recorded in the machine before applying a major load. The hardness value of the specimen can be obtained from the total difference of the depths indenter ($\Delta H = H_1 - H_2$). Therefore the equation (2.2) about the hardness value can be determined as follows:

$$HRX = M - \frac{\Delta H}{0.002} \quad (2.2)$$

where M is the maximum scale which equals 100 in general for testing with the diamond indenter with scale A, C and D. Then, where ΔH is $(H_1 - H_2)$ the total difference of the depths indenter on the specimen's surface. Lastly, the result of hardness value can be converted into tensile strength value by using the conversion table of Rockwell hardness value.

2.5 Fatigue Failure Analysis

Mechanical component can be effected by cyclic loading that can cause fatigue failure which normally occurred below the ultimate strength of a material. Most recently (Zhi-Wei Yu, 2015) has studied the cyclic loading causes a progressive degradation of the material properties and eventual failure. Obviously, the role of an engine mount component is to isolate the vibration and reduces dynamic force. Therefore, the vibration analysis is conducted to determine the value of vibration transmissibility, elastic stiffness and force applied. The results will give information about the performance of mount before consider it in design stage. Hence, the design of engine mount component must be detailed and précised in order to make component successfully function within some performance parameter ranges. However, the failure of engine mount component typically at the elastic element or part. The elastic elements which are stiffer and damping in mount system use the material such as elastomeric rubber for its high stiffness and stability. Since then, there are many design proposal used elastomeric mount to isolate vehicle structure from engine vibration source (Heisler, 2002). Basically, the development of elastomeric engine mount component has been conducted using the physical prototyping and testing techniques. There are two types of static structural testing conducted in order to determine the behavior and performance of an engine mount component which are by conducting experiment and finite element analysis (FEA).

2.5.1 Experimental

In order to determine the behavior of elastomeric rubber, it needs to perform an experiment test to obtain the material stress-strain curves for a certain mode of deformation. The experimental information using a least squares fit procedure which minimizes the relative error in stress result (J.C.Snowdon, 1968). Therefore, the elastomeric materials must be tested on various loading conditions that can describe the behavior of the material. There are two types of experimental set up used to obtain the static load displacement curves (Amos, 1930) shown in Figure 2.7. The experiment on the mount component very important in the design procedure to ensure the safety and reliability of rubber component.



Figure 2.7: Experimental Test Conduct in A) Longitudinal and B) Transversal Direction

Source: (Amos, 1930)

2.5.2 Static Structural Analysis Model

The FEA is widely used in engineering field especially in structural engineering. Generally, it is a numerical method for solving engineering problem with loading and material properties. Moreover, using the finite element analysis model of the mount component that best described the behavior of the elastomeric material with various loading applied. The flow chart in Figure 2.8 shows the action or step for the static structural analysis by using FEA.

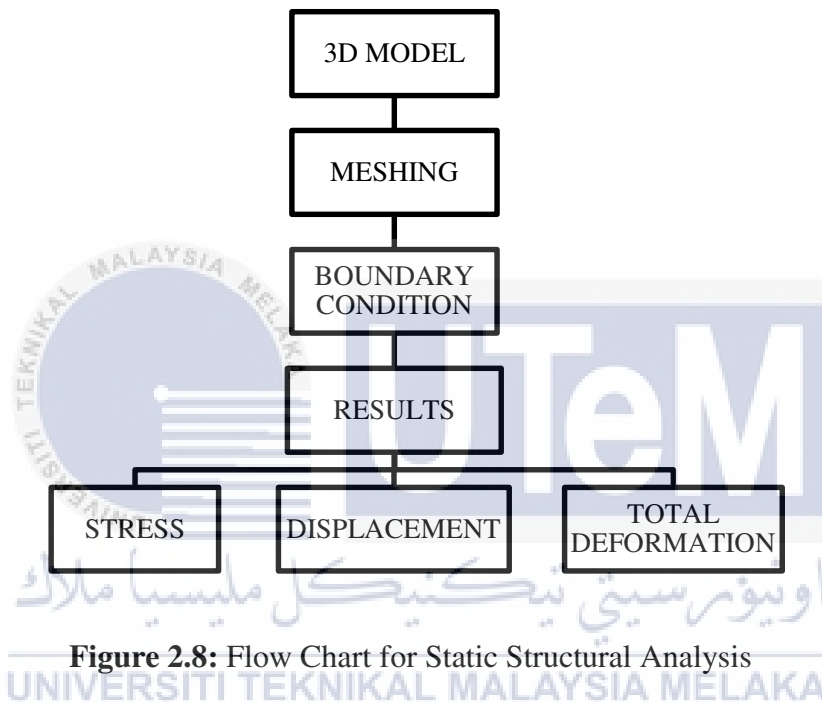


Figure 2.8: Flow Chart for Static Structural Analysis

2.6 Fatigue Failure under Cyclic Stress

It has been discussed earlier that the main objectives of this project is to investigate the influence of cyclic stress and thermal loading on an engine mounting component. An engine mount component has been continuously investigated which may lead to structural failure by the cyclic loading. A failure by cyclic stresses or fatigue is a form of failure that occurs in structures subjected to dynamic stresses over an extended period. This characterized by maximum and minimum stresses, mean stress and stress amplitude. The effect of zero mean stress is accounting in fatigue analysis for many service load histories, which means that the load cycle is completely reversed (Qasim, 2014). A zero mean stress is shown in Figure 2.9 is generated as fatigue data. Moreover, a zero mean stress is also called completely reversed cycling and corresponds to $R = -1$.

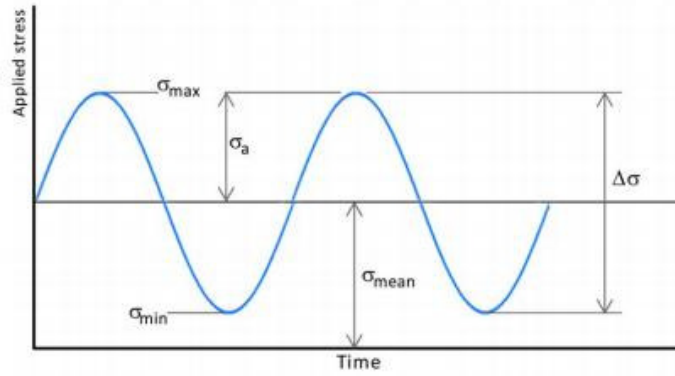


Figure 2.9: Constant Amplitude Loading

The following equations are used to define a stress cycle with both mean and alternating stresses in fatigue analysis. The equations (2.3) – (2.8) can be used in methods for estimating mean stress effect that correlate with stress life curve data.

Constant Stress Range:

$$\Delta\sigma = \sigma_{max} - \sigma_{min} \quad (2.3)$$

Mean Stress:

$$\sigma_m = \frac{\sigma_{max} - \sigma_{min}}{2} \quad (2.4)$$

Stress Amplitude:

$$\sigma_a = \frac{\Delta\sigma}{2} = \frac{\sigma_{max} - \sigma_{min}}{2} \quad (2.5)$$

Stress Ratio:

$$R = \frac{\sigma_{min}}{\sigma_{max}} \quad (2.6)$$

Maximum Stress:

$$\sigma_{max} = \sigma_m + \sigma_a \quad (2.7)$$

Minimum Stress:

$$\sigma_{min} = \sigma_m - \sigma_a \quad (2.8)$$

Where $\Delta\sigma$ is stress range, σ_{max} and σ_{min} are maximum and minimum stress under constant amplitude loading. A boundary condition of stress state as a function of stress amplitude σ_a , the mean stress σ_m and chosen material parameter beyond which material will be destroyed.

2.6.1 S-N Curve

The fatigue life of a component can be determined by using the alternating stress amplitude (σ_a) versus number of cycles (N_f) to failure, which is typically known as S-N curve. The example of the S-N Curve for steel is shown schematically in Figure 2.10. Generally, the constant amplitude S-N Curve of this type is plotted on semi-log or log-log coordinates. A fatigue limit or endurance limit (S_e) represents a stress level below which the material does not fail and can be cycled infinitely. After that, the Goodman-Line is a method used to estimate the influenced of the mean stress on the fatigue strength (Jadav Chetan, 2012). The S-N curve is developed by a series of sample tested to failure at various stress ranges. However, the constraint using the S-N Curve is that the resulting plot is highly dependent on the test conditions. The test condition can be influenced by many factors such as the stress ratio, sample of material geometry and surface condition of the test specimen. This severely limit the application of the S-N Curve.

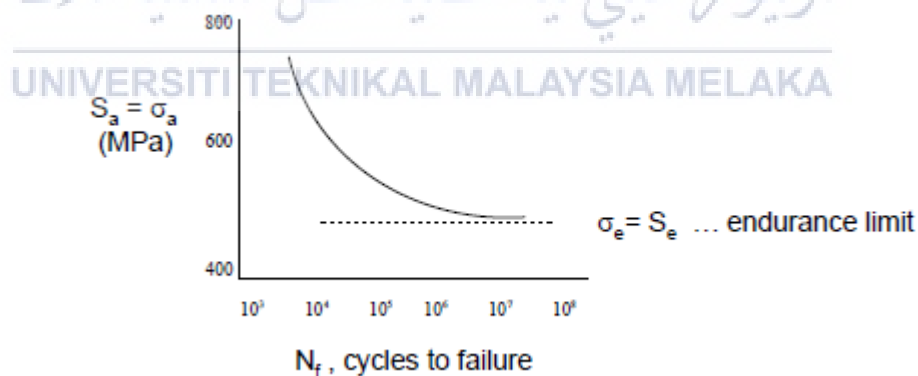


Figure 2.10: S-N Curve for Fatigue Life Evaluation

Therefore, the S-N curve is a graphical representation of fatigue data that shows the relationship between fatigue life in cycle when stress amplitude is applied. Basically, the Basquin's equation is the most commonly used as analytical expression for finite life (Krzysztof Kluger, 2013). Based on the equation (2.9), the life prediction can be done:

$$\sigma_a = a N_f^b \quad (2.9)$$

where σ_a is the fatigue stress amplitude (MPa), N_f is the number of cycles to failure (MPa), a is constant ($1/15 < a < 1/8$) and b is fatigue strength exponent used for calculation of fatigue life of the metallic materials.

2.6.2 Goodman Diagram

Generally, there are many theories can be used to study the influence of mean stress to predict fatigue life under fluctuating loading which are the Goodman theory, Soderberg theory and Gerber theory (M. R Ayatollahi, 2011). In this study, it was decided that the Goodman theory will be employed to predict fatigue life of an engine mounting component. The Goodman theory has been expressed in mathematical expression as the following:

$$\frac{\sigma_a}{\sigma_e} + \frac{\sigma_m}{\sigma_u} = 1 \quad (2.10)$$

where σ_a the alternating stress, σ_e is the endurance limit, σ_m is mean stress and σ_u is the ultimate strength of the material. Then, a Goodman diagram defines as a failure surface for varying mean stress. Basically, a Goodman diagram is constructed by plotting the mean stress on the X-axis and alternating stress on the Y-axis as displayed in Figure 2.11.

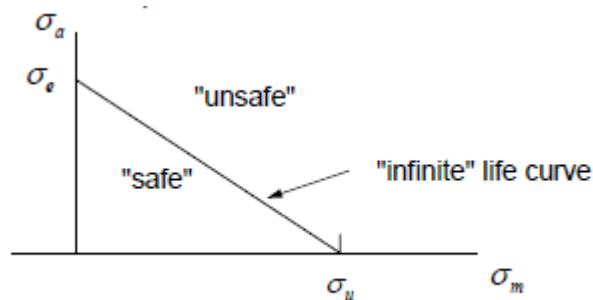


Figure 2.11: Goodman Diagram

A Goodman diagram at the first point on the line is plotted at a mean stress (σ_m) of zero in magnitude and an alternating stress (σ_a) equal to the endurance limit (σ_e). Then, the second point is an alternating stress of zero and a mean stress is equal to the ultimate tensile stress (σ_{ult}). Hence, a straight line from the connecting points defines the Goodman line. Lastly, a Goodman line can also predict whether an engine mounting component is under safe or unsafe condition. If any point that falls below the Goodman line as shown in Figure 2.11, the component is safe and above the Goodman line a component is considered unsafe or will eventually fail.

2.7 Material

A growing trend in the field of automotive, component needs for light weight structural material for improvement in emissions and fuel consumption (G.S. Cole, 1995). Then, the selection of the material must be considered at design stage of an engine mounting components. However, the mechanical properties of the material is important to make the product in feasibility and adaptability and function effectively (Tushar Tandon, 2015). Lastly, the two type of material used in this study are AISI/SAE 4130 as the structure and the elastomer (Butyl Rubber) material as the stiffness element of the engine mounting component.

2.7.1 AISI/SAE 4130 steel

The AISI/SAE 4130 steel has been widely used for automotive parts because it is light weight material. Then, the AISI/SAE 4130 steel grade is a versatile alloy with good atmospheric corrosion resistance and reasonable strength up to around 315 °C. Moreover, the steel shows high strength and toughness, higher resistance to corrosion, excellent weldability and higher fatigue strength (Chawla, 1993). Then, the steel commonly referred to as a chrome moly steel, containing nominally 0.28-0.33% Carbon, 0.8 – 1.1 % Chromium and 0.15– 0.25% Molybdenum. The steel generally similar with 4140 steel which has a higher carbon level (0.28-0.33 %). The tensile strength is 560 MPa, the yield strength is 460 MPa and the Poisson's ratio is 0.27. Lastly, the AISI/SAE 4130 steel has been selected for simulation purpose due to its mechanical properties that closely similar to the properties of the actual engine mounting component.

2.7.2 Elastomer (Butyl Rubber)

An engine mounting system the material that used is elastomer because the material has an ideal dynamic stiffness and a high damping element to prevent the engine leap and ensure the vehicle in stability condition. Then, the function of mounts element is to act as a vibration isolators and provide damping. The used of elastomer material is to give a high stiffness and provide support to the engine system. Therefore, the good stiffness element material can affect their characteristic behavior when it is subjected to load and temperature (Peng Wang, 2005).

In this study the elastomer (Butyl Rubber) is used for the FEA simulation purpose because the material generally use in anti-vibration mount application. The composition of this material is typically 98% polysobutylene and 2% isoprene. Then, the Bultyl rubber has a typical service temperature range between 59 °C – 121 °C. The tensile strength is 7.5 MPa and the yield strength is 2.5 MPa with density of 0.9 Mg/m³ and the Poisson's ratio of 0.27.

2.8 Manufacturing Process

The design of an engine mounting component comes in variety of shapes and sizes depends on the manufacturer and to meet variety of needs. Most of the engine mounting component consist of structural body and stiffness element. In this study, the engine mounting component consist of several parts as shown in Figure 2.12. In addition, there are fabrication process involves in the engine mounting which are metal bonding process and welding process. The rubber to metal bonding must be designed to handle with high pressure, harsh environmental condition and extreme temperature to ensure a permanent seal of the bonded components long lasting. Lastly, the welding process joints the metal rod and metal mount frame while the rubber-metal bonding process connects elastomer and metal.

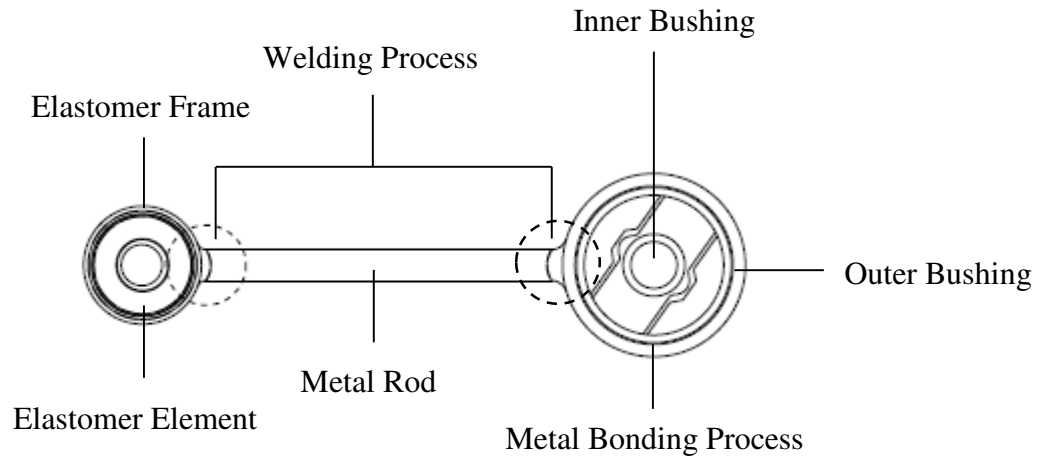


Figure 2.12: The Specification of Engine Mount Component

2.8.1 Rubber to Metal Bonding Process

Generally, rubber to metal bonding is an ideal process for bonding metal and plastic parts such as roller, engine mount, shock absorber, shafts seal. Then, the main field of application for the components are made with rubber to metal bonds. In the automotive industry, metal bonding process is used to connect the elastomer and metal. The rubber bonding process which rubber is mechanically bonded to a metal by insert the rubber during the molding process (Violettle, 2003). Then, the high quality bonded parts begins with two elements which are the elastomer material and the adhesive system. But, the essential element is the adhesive system which is the rubber bonding agent. The selection of bonding agent depends on the type and modulus of elastomer rubber. The bonding agent must have a higher strength compared to durability and resistance to environmental factor such as oil, temperature and chemical. The rubber to metal bonding agents usually contain a mixture of resins, polymers, extender and corrosion inhibitors. Lastly, the wide range applications of rubber to metal bonding has to meet the requirement of the environmental pressure and physical demand.

2.8.2 Welding Process

Basically, a comprehensive variation of automobile body components are joined together using welding process. The welding technique demands for improved productivity, quality and efficiency of the components. After that, the automotive manufacturers mostly focused on producing on lighter and strong structural of vehicle car body to make high fuel efficiency. The fabrication of the strong structural member can be achieved by using the welding technique. The purpose of a welding technique is used to make permanent joint between two metals with suitable combination of pressure, temperature and metallurgical compliant. Hence, (Devarasiddappa, 2006) states that the type of the welding that most commonly used for automotive application includes resistance seam welding (RSEW), plasma arc welding (PAW), friction welding (FW), laser beam welding (LBW), tungsten inert gas (TIG) and metal inert gas (MIG). Lastly, the selection of the best type of welding process for the automotive component depends on the working condition of the welded part.

2.9 Finite Element Analysis (FEA)

Finite Element is used to express the mechanical behavior of a structure in finite element analysis. It became a useful method in numerical solution of a wide range of engineering problems. The analysis that can be done includes the deformation and stress analysis especially in term of total stress (Von-Mises Equivalent Stress) in automotive, aircraft, building, structures and including the analysis in thermal heat such as flux, fluid flow, magnetic flux and other flow problems.

FEA is practically the numerical technique to solve engineering problem. FEA is useful for problem with complicated geometries, loadings, and material properties where analytical solutions cannot be obtained. According to (Ramamurty, 2010), the purpose of FEA is to make the analytical solution or stress analysis for trusses, beam, and other simple structures are carried out based on dramatic simplification and idealization.

Performing structural analysis requires a complete information for the structure such as structural loads, condition of supports and material properties. The result of analysis

usually includes support reaction, stresses and displacements. All of the information gained and compared to the criteria in order to indicate with the failure conditions.

2.9.1 ANSYS Software

ANSYS software is one of the engineering software that has the capability to solve the engineering problem especially on numerical method problems. ANSYS Software is a comprehensive software that spans the entire range of physics by providing an access to virtually any field of engineering simulation that a design required. The structural analysis have special relations with the applied mechanics, material science and applied mathematics to compute the structures deformation.

In the industry, ANSYS is the software that can do the analysis to solve the complex problems such as aerospace, automotive, heavy equipment or machinery, bridges and buildings. For the structural analysis problems, ANSYS provided to solve the complex structural engineering problems such as linear statics analysis that simply provided stresses and deformation that involving dynamic complex behaviors.

2.9.2 Modeling on Finite Element Analysis (FEA)

Analysis on Finite Element (FE) can be used to simulate the structural problem by 1D (one-dimensional), 2D (two-dimensional) and 3D (three-dimensional) of the elements. At first, the 1D (one-dimensional) element been developed to carry out in Finite Element (FE) analysis. But, the great capability of Finite Element through time especially in solving complex engineering problems brings up 2D (two-dimensional) and 3D (three-dimensional) elements, the expected result on the analysis will be more accurate and provide improvement on the complex modelling. It also brings improvement on the evaluation of numerical problem, results validation and computer capabilities on solving the complex problems.

2.9.2.1 One Dimensional (1D) Element Modelling

In the Finite Elements, 1D (one-dimensional) is the earliest element that has been introduced to solve the structural problems. Usually, it is built in the form of one straight line or curve line which is call 1D line element.

The connection of the simple 1D element is through two nodes. The example of 1D elements are truss element, bar element and beam element.

2.9.2.2 Two Dimensional (2D) Element Modelling

The 2D elements, it has surface with the basic shape are quadrilaterals or triangle. Generally, it connects at common nodes along common edge to form continuous structures. Moreover, 2D element is important because it can be used to analyze under the plane strain and plane stress conditions. Usually, the 2D structural elements are often used to solve 2D elasticity problem. The 2D structural elements are 4 nodes, 10 nodes for tetrahedral element and 8 nodes for isoperimetric as shown in Figure 2.13.

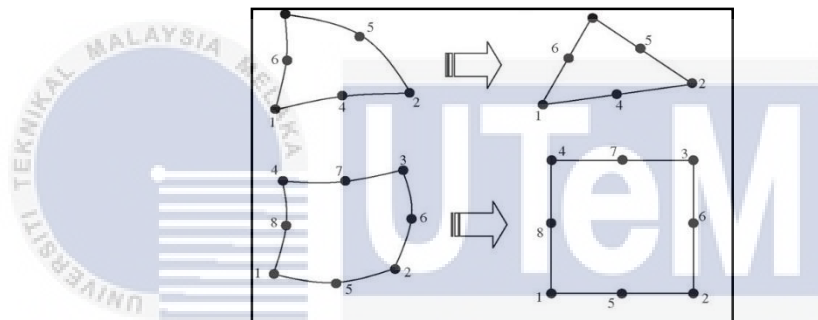


Figure 2.13: Two Dimensional (2D) Element Modeling

Source: (Kumar, 2008)

2.9.2.3 Three Dimension (3D) Element Modelling

The 3D (solid) element is modelled to solve the problems in volumes with meshing. Thus, 3D element also depend on the degree of freedom of the structures. Figure 2.14 shows the three dimension (3D) element modelling used in finite element analysis and this type of modelling will be used in the project.

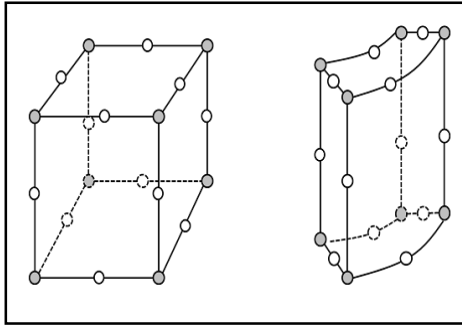


Figure 2.14: Three Dimension (3D) Element Structures

Source: (Kumar, 2008)

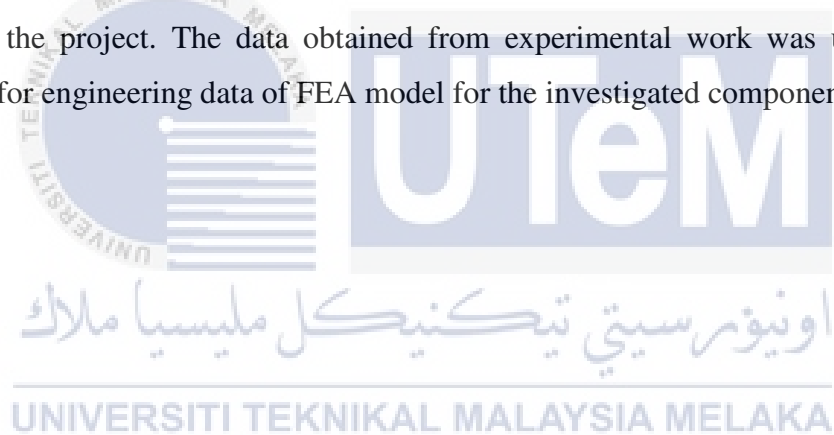


CHAPTER 3

METHODOLOGY

3.1 Introduction

This chapter covers the research methodology with detail description of the entire work of this project. The most important thing that needs clarification here is the procedure regarding the objective of the project is to validate the result by comparing result from ANSYS software with the theoretical calculation for fatigue analysis. This chapter will be divided into several sections which will describe the experimental work and simulation analysis of the project. The data obtained from experimental work was used to set as parameters for engineering data of FEA model for the investigated component.



3.2 Project Flow Chart

The flow chart of the current project is shown in Figure 3.1. It will clarify all the procedures in order to achieve the project's objective.

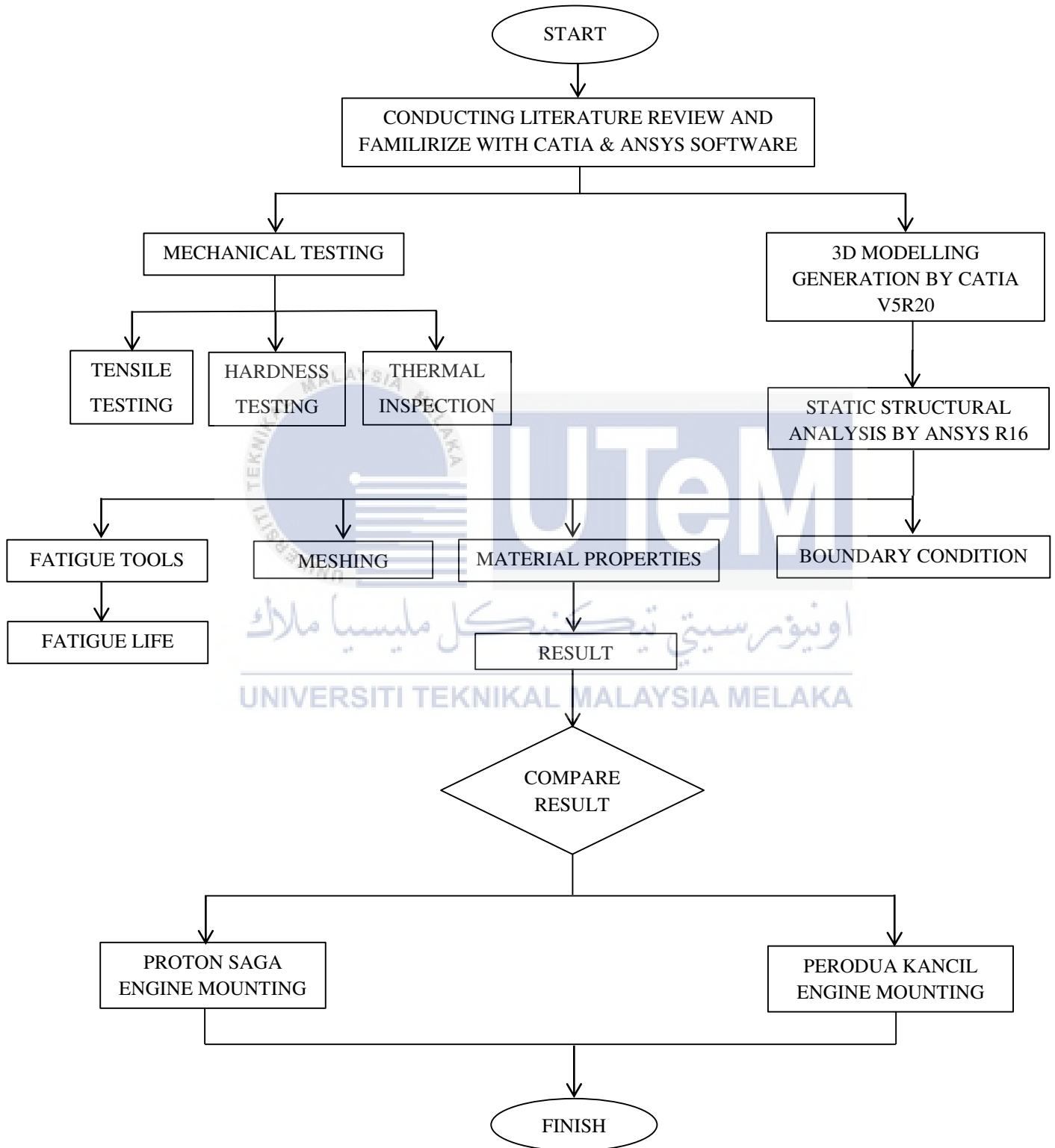


Figure 3.1: Project Flow Chart

3.3 Development of Experiment

In this section, the development of experiment is discussed. The details of process from the early stage until the end will also be discussed. Finally, the results of mechanical test which are tensile test, hardness test and inspection of temperature on engine mounting component will be shown.

3.4 Tensile Test

This tensile test was carried out to determine the mechanical properties of the metallic part of engine mounting component. The tensile test is used to obtain material's information that will be used in FEA simulation analysis with the requirement of the appropriate specification. The objective of this test is to observe and evaluate the mechanical properties of steel for the engine mounting under tensile loading. The applicable document for the testing is ASTM E8 (ASME-E8, 2003) which is standard tension testing of metallic materials. The reference standard is used for the preparation the dimension specimen and the procedure of the testing.

3.4.1 Theory

Tensile test is one of the most widely used testing to determine mechanical properties of metallic material. This test is done by gripping the ends of a standard test piece of tensile test. Then, applying a continually increasing uniaxial load or force until failure occurs on a test specimen. Moreover, tensile test can be used to determine properties such as yield strength, percent of elongation, tensile strength and other material properties.

3.4.2 Test Specimen

The test specimen consist of a round cylinder 8.86 mm diameter by 105 mm in length. The total length of the specimen as required by the standard shall be at least equal to the gage length plus the length of material required for the full use of the grips employed. The specimen follow the ASTM E8 standard is shown in the Appendix A in order to make results are reproducible as shown in Figure 3.2. The detail dimension of the specimen shown in the Appendix B.

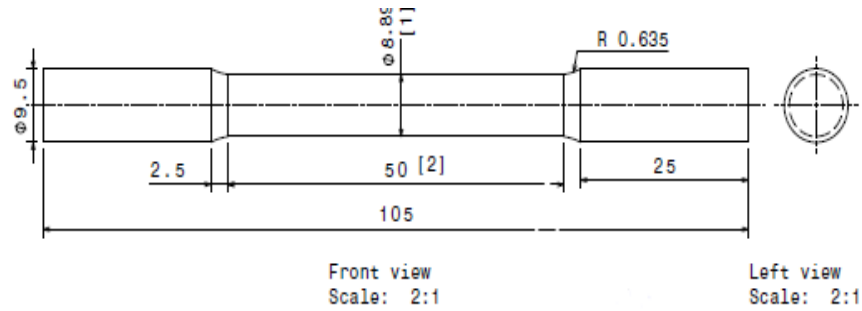


Figure 3.2: Round Tension Test Specimen

3.4.3 Procedure

The test specimen was conducted at $23 \pm 2^\circ\text{C}$ $50 \pm$ relative humidity as required by the ASTM E8-04. The three dog bone shape testing specimens were prepared. The original length and diameter was marked to calculate the percentage of elongation and reduction. The marking position was at three different places within gauge length area to get the average of the test results. The initial gauge length (grip separation) at 12.5 mm and the rate of stressing or loading at 11.5 MPa/s were set. The specimen should be aligned as perfectly as possible with the direction of the pulling load. The specimen was aligned with the axis where it was gripped by the upper and lower clamp of the testing machine. After that, the test was started and the load versus extension was recorded by the computer. The testing steps were repeated on all three specimens. Lastly, the graph of load versus extension was used to calculate the Young's modulus, yield strength, ultimate tensile strength, fracture strain, percent of elongation and percent reduction of area of the broken specimen and the data were tabulated in the table.

3.4.4 Theoretical Formula

Tensile strength or ultimate tensile strength is calculated by dividing the maximum load obtained from the tensile test graph by the original cross-sectional area, A_0 . The result is expressed in Mega-Pascal (MPa) and reported to three significant figures. The equation 3.1 defines tensile strength as:

$$\text{Tensile Strength} = \frac{(\text{maximum load})}{\frac{\pi d^2}{4}} \quad (3.1)$$

The percent of elongation is calculated by dividing the elongation at the moment of rupture by the initial gauge length and multiplying by 100. The percentage of elongation after fracture is given by equation 3.2 and the equation 3.3 defines the percentage reduction of area.

$$\text{Percent Elongation} = \frac{(l_f - l_o)}{l_o} \times 100\% \quad (3.2)$$

$$\text{Percent Reduction in area} = \frac{(A_o - A_f)}{A_o} \times 100\% \quad (3.3)$$

where l_o is the original gauge length, l_f is the final gauge length, A_o is the original cross-section of area and A_f is the minimum cross-sectional of the specimen after finishing the testing.

Young's Modulus is calculated by drawing a straight line tangent to the initial linear portion of the stress-strain curve. The result is expressed in Giga-Pascal (GPa) and reported to three significant figure. The Young's Modulus is calculated by using equation 3.4.

$$\text{Young's Modulus, } E = \frac{\Delta\sigma}{\Delta\varepsilon} = (\text{Slope of linear part}) \quad (3.4)$$

Yielding occurs at the beginning of plastic deformation by considering the stress-strain curve beyond the elastic portion. The yield strength is calculated by using equation 3.5.

$$\text{Yield Strength, } \sigma_y = \frac{P_y}{A_o} \quad (3.5)$$

where P_y is the load at yielding and the A_o is the original cross-sectional area of the specimen.

3.4.5 The Results of Tensile Test

For all three specimens used in the tensile tests, the data of its initial gage length and diameter before and after failure are tabulated in Table 3.1. The data is used for calculation the percent of the elongation and reduction of area of the failed specimen. The average final length is 55.38 mm become longer compare to original length is 50 mm because of elongation. The average final diameter is 6.07 mm become smaller because of the reduction of the cross section of area.

Table 3.1: Detailed Tensile Test Specimen Dimensions

Nominal Diameter	Specimen 1	Specimen 2	Specimen 3	Average
Initial Gage Length, mm	50	50	50	50
Final Gage Length, mm	55	56.13	55	55.38
Initial Diameter, mm	8.8	8.83	8.7	8.78
Final Diameter at fracture	6.4	6	5.8	6.07

Figure 3.3 shows the result of the final gauge length of specimen after test. This figure showed that the fracture occur at the grip of the specimen not at the middle of the gauge length as expected. The fracture occurred at grip region because the diameter of the test specimen was found not uniform as a result of the machining work.



Figure 3.3: Gauge Length at Failure of Specimen 1

After finishing the tensile test the data from the test was plotted on one graph for the three specimens of engine mounting component. The average value of the three results is used as the final result of the test. Figure 3.4 shows the stress-strain curves of all three tests.

Stress-Strain Curve

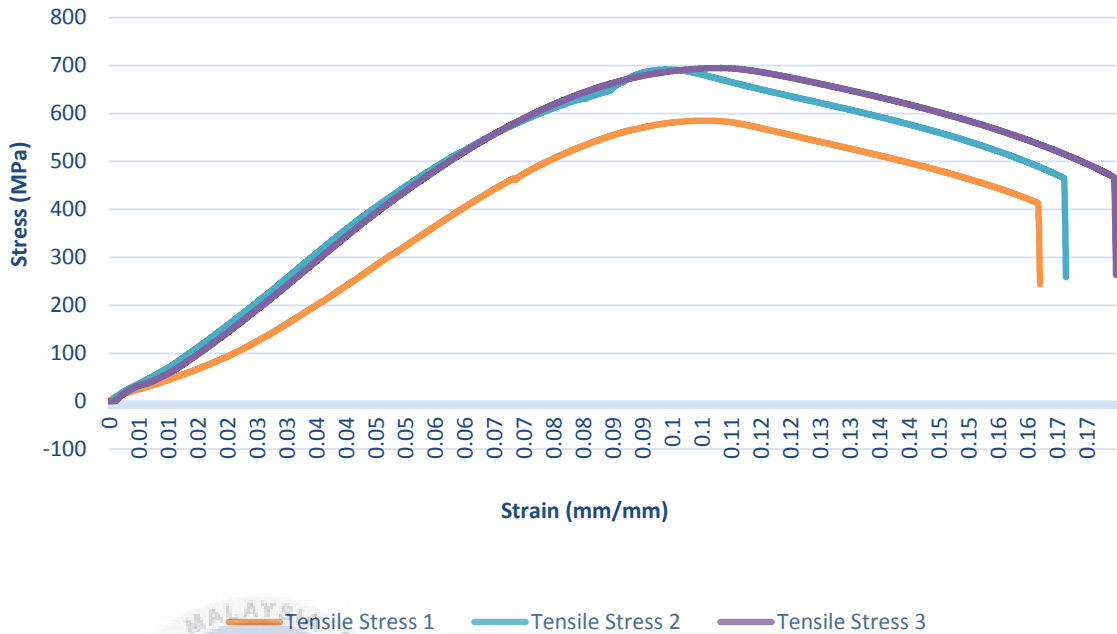


Figure 3.4: Result Tensile Test of Three Specimen

In this graph stresses were plotted along the vertical axis and the strain are plotted along the horizontal axis. The average value of the ultimate stress point about 704 MPa that show the maximum strength of the material have to bear before breaking. The average value of yield stress is 505 MPa that defined the material yields at this value. Generally, the yield strength represents the initiation of permanent deformation of the specimen where the material experienced plastic deformation until it fails.

The accuracy of tensile test results very much depends on the method of specimen preparation, accuracy in measurement of specimen dimensions and method of measuring extension. Moreover, the tensile strength and elongation results are also influenced by the initial history of the material and any invisible flaws in the specimen. However all these factors must be carefully controlled in order to get results with high accuracy and reliability.

3.4.6 Material Properties

The final result of the tensile test for each specimen is listed in Table 3.2. The detail result of tensile test for the three specimen components is shown in Appendix C. The stress corresponding to the ultimate tensile strength is where necking begins to occur. From the test, the yield and tensile strengths, the percentage of elongation and the percentage of reduction in area were determined using the theoretical method described in section 3.4.4 is shown in Appendix D.

Table 3.2: Experimental Results of Tensile Test for Three Specimen

Detailed	Specimen 1	Specimen 2	Specimen 3	Average
Tensile Strength (kN)	44.15	42.36	41.31	42.61
Ultimate Tensile Strength (MPa)	725.90	691.74	694.91	704.18
Extension at Break (mm)	8.21	8.44	8.88	8.51
Yield Strength (MPa)	526.13	535.98	454.19	505.43
Fracture Strength (MPa)	510.51	464.75	458.06	477.77
% Elongation	10 %	12 %	10%	10.7%
% Area of reduction	27.3 %	32.2 %	33.3 %	30.90 %

The average value of the yield strength is greater than 500 MPa and the average value of ultimate strength is greater than 700 MPa. It can be concluded that based on the mechanical properties obtained through the tensile test the material is AISI/SAE 4130. Lastly, the appearance of fracture surface for the specimen after testing is cup and cone shape as shown in Figure 3.5, which is a typical fracture behaviour of ductile material.



Figure 3.5: The Cup and Cone Fracture Behaviour of a Ductile Metal

3.5 Hardness Testing

The present study used the Rockwell hardness testing on the specimen engine mounting component. It can provide useful information about physical and mechanical properties of the engine mounting component. This information may correlate to tensile strength, wear resistance, ductility and other physical characteristics of metallic materials. A primary aim is to measure the Rockwell Hardness values of materials and estimate the ultimate tensile strengths by the aid of conversion tables. This experiment used the ASTM E18 (ASTM_E-18, 2012) standard for test methods for Rockwell hardness of metallic materials.

3.5.1 Theory

The hardness test is the most valuable and widely used mechanical test for evaluating the properties of the metals as well as certain other materials. Moreover, the hardness of the material usually is considered resistance to permanent indentation. The Rockwell hardness test using a verified machine to force a diamond indenter under specified conditions. Generally, an indenter is pressed into the surface of the metal to be tested under a specific load for measurement the hardness of the material. The hardness value will be displayed on a dial or a screen by having 100 divisions and each division represents a depth of 0.002 mm. Therefore the hardness value can be determined from an equation 3.6.

$$HRX = M \frac{\Delta H}{0.002} \quad (3.6)$$

where ΔH is $H_1 - H_2$ and M is the maximum scale which is equals to 100 in general for testing with the diamond indenter (scale A, C and D). The testing procedure starts with indenting a flatly ground metal surface with diamond with minor load 98N to position the metal surface as shown in Figure 3.6,

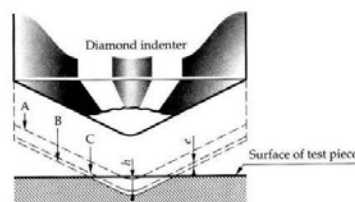


Figure 3.6: Rockwell Hardness Tester Indenter

where A is the initial position of indenter under pre-test load, B is the position of indenter under total test load, C is the position of indenter under pre-load after removed total test load and h is the permanent depth of indentation.

3.5.2 Test Specimen

This report measuring hardness on the specimen engine mounting component using the type static indentation test. The test using a cone type that is forced into the surface of the specimen that being tested. The relationship of load to the area or depth of indentation is the measure of hardness. Lastly, the test specimen should be smooth, free from oxide scale, foreign matter and lubricant.

3.5.3 Procedure

The specimen material was placed at the anvil of the hardness tester, the suitable gripped was used because the specimen round shape as shown in Figure 3.7. Then, the indenter was brought into the contact with the test surface that the direction is perpendicular to the surface. The preliminary test force F_0 is 98N was applied. The force F_0 is 98N was used because more suitable for the hardened steel material as shown in Table 3.3. In this hardness test, a 120° diamond cone indenter was used because this type of indenter used for HRC test. The value of the additional test force F_1 was increased and the total value test force give hardness scale. The value force F_1 was increased to obtain the required total test force F. Lastly, the result of Rockwell hardness value was calculated and the value of hardness were converted to the tensile strength using the conversion table.



Figure 3.7: Setup of Hardness Test

Table 3.3: Rockwell Hardness Scales

Scale Symbol	Load	Preload	Indenter	Typical Application
HRC	98 N	980 N	120° diamond cone	Steel, hard cast irons, malleable iron and deep case hardened steel

3.5.4 Hardness Test Results

The hardness test of engine mounting component specimen was performed in the Laboratory of Material Science. The results obtained of Rockwell (HRC) and the average of the measurement are shown in Table 3.4. The total average of the three specimen is 9.67 and by using the hardness conversion table it is equivalent to 640 MPa for the tensile strength of the test material. This method of defining strength based on the HRC result gives 9.2% less than the result of tensile strength as obtained through the tensile test previously shown in Table 3.2. The lower value of σ_{ult} gained through the hardness data maybe depending on the size and shape of the test pieces, manufacturing of material, metallurgy phases and their locations to be analyzed. Lastly, the hardness data may also be used for estimating other related mechanical properties of the materials.

Table 3.4: Results of Hardness Test

Specimen	Reading 1	Reading 2	Reading 3	Average
1	10.5	8.9	9.5	9.6
2	9.0	9.3	10.5	9.6
3	9.7	10.0	9.6	9.8
Total Average				9.67
Tensile Strength (MPa)			640 < 705 (Tensile Test)	

Note: The hardness conversion table can be found in Appendix E.

3.6 Thermography Inspection

The study of thermography inspection was carried out on the engine mounting component under real condition. The thermography also called infrared inspection is based on the sensing of heat emitted from an object in the form of infrared radiation. The thermography measures surface temperature by using infrared camera on the devices. After that, the resulting images will determine the average value of maximum and minimum heat on the component. The inspection was performed on Proton Saga vehicle while travelling about half an hour on road surface. The inspection was repeated three time and the average value was tabulated in a table. The actual temperature is measured by using the FLIR thermal camera. The inspection can observe the physical phenomena and thermal change of the component. The objective of this inspection is to observe and determine the value of temperature at critical point of the engine mounting component. The information of the temperature data from the inspection will be used in simulation analysis study.

3.6.1 Thermography Result

The target location of the thermal camera was determined based on the most critical failed area on engine mounting component. The car was travelled for about half an hour on road surface. Hence, the three locations of the engine mounting camera were captured using the FLIR thermal camera as shown in Figure 3.8.

Table 3.5: Temperature Data of Engine Mounting Component

Image Info	Part A	Part B	Part C
Background temperature	38.0 °C	38.0 °C	38.0 °C
Emissivity	0.95	0.95	0.97
Transmission	1.00		
Min Temperature	34.44 °C	33.89 °C	35.00 °C
Average Temperature	47 °C	46.94 °C	47.17 °C
Max Temperature	60.53 °C	60 °C	55.17 °C
Image Range	34 °C to 60.5 °C	33.33 to 60 °C	32.39 °C to 54.17 °C
Camera Model	Fluke Ti32		
IR Sensor Size	320 x 240		
Camera serial number	Ti32-10070187 (9Hz)		
DSP Version	1.2.19		
OCA Version	1.2.19		
Camera Manufacturer	Fluke Thermography		
Calibration Range	-20 °C to 600°C		
Severity	None		

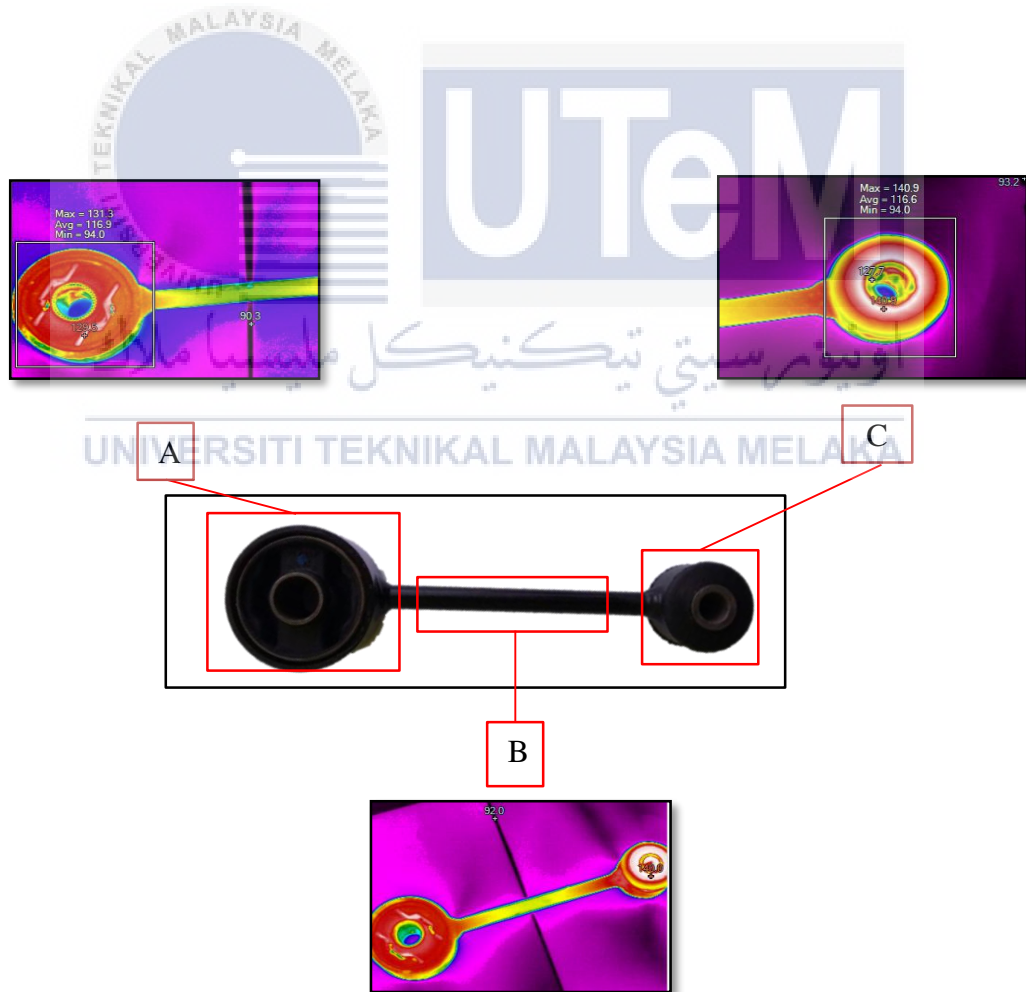


Figure 3.8: The Thermal Imaging Inspection on the Component

Based on the measured data shown in Table 3.5 it shows the variation of temperature at three point of critical area of the component. The thermography inspection find the maximum temperature is 61 °C and the minimum temperature is 35 °C. After that, the total average temperature of component is 47°C.

3.7 Generation of CAD Model

For this project, the static analysis will be performed for the existing engine mounting component with all constant dimensions. Normally, an engine mounting component consist two type of material, known as structure steel frame body and elastomeric stiffness element. A three dimensional (3D) CAD model is generated using the commands in CATIA V5R20 software. Then, parametric generation of drawings shown in Appendix F and Appendix G will help to get the details dimensions useful in forces calculations under cyclic stresses and thermal loading on a component. The modelled components are exported to IGES format, which is able to retrieve by ANSYS for the pre-processing of the part. The CAD model of an engine mounting component by different manufactures are shown in Figures 3.9 and 3.10 for the Proton SAGA and Perodua KANCIL respectively.



Figure 3.9: Isometric View (3D) model of PROTON SAGA Component

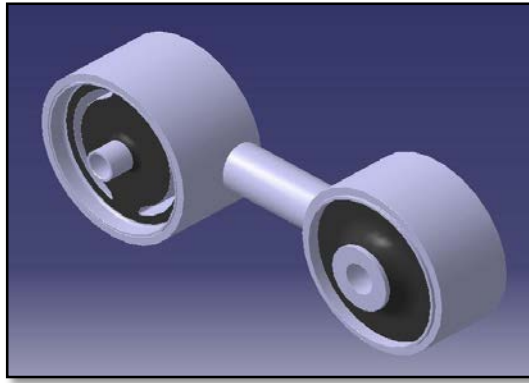


Figure 3.10: Isometric View (3D) model of PERODUA KANCIL Component

3.8 Static Structural Analysis

The condition of the equilibrium of the bodies acted by forces deals with static structural analysis. Then, a static analysis is used to determine the stress, strain, and total displacement in a component parts. There are various types of loading that can be applied in this analysis included externally applied forces and temperatures loading. However, a static structural analysis required information for analysis such as material properties, meshing and boundary conditions. Figure 3.11 shows flow chart for the structural analysis method using FEA, as used in this study.



Figure 3.11: Flow Chart of the Structural Analysis Method

3.8.1 Material Properties

The materials used for an engine mounting components consist of AISI/SAE 4130 Steel and Butyl Elastomer since its material properties were close to that of actual material. The material properties of AISI/SAE 4130 Steel and Butyl Elastomer are listed in Table 3.6 and Table 3.7. However, the fatigue analysis need to set the finite life value that will be used as the S-N curve for the AISI/SAE 4130 steel material.

Table 3.6: Properties of AISI/SAE 4130 SteelMaterial Properties

AISI/SAE 4130 Steel

Material Property	Value
Young's Modulus (E)	210 GPa
Poisson Ratio (ν)	0.29
Yield Stress (σ_{yield})	505 MPa
Ultimate Tensile Stress (σ_{ultimate})	704 MPa
Density (ρ)	7.85 g/m ³
Thermal Conductivity	42.7 W/m.K

Table 3.7: Properties of ElastomerStiffness Element

Butyl Rubber

Property	Value
Young's Modulus (E)	0.0015 GPa
Poisson Ratio (ν)	0.3
Yield Stress (σ_{yield})	2.5 MPa
Ultimate Tensile Stress (σ_{ultimate})	7.5 MPa
Density (ρ)	0.91 Mg/m ³
Coefficient of Thermal Expansion	130 x 10 ⁻⁶ mm/mm °C

The fatigue tool will use the information from the S-N curve for the AISI/SAE 4130 steel material. However, the ultimate tensile stress and yield stress based on the tensile test that was conducted on the material of engine mounting component. The fatigue properties used in this study are listed in Table 3.8. The graphical representation of the S-N curve data is shown in Figure 3.12 for the steel material. The graph shows the alternating stress value is reducing with number of cycles. Then, fatigue limit corresponding to one million cycles represented by 282 MPa for the material. So, fatigue analysis is carried out for this endurance limit with the high cycle region is considered. Moreover, fatigue life is specified for one million cycles which is defined with endurance limit of the material under reversed loading.

Table 3.8: Properties of Alternating Stress Mean Stress

Fatigue Tool

AISI/SAE 4130 Steel

Property	Value
Interpolation	Log-Log
Scale	1
Curve Type	Stress-Life

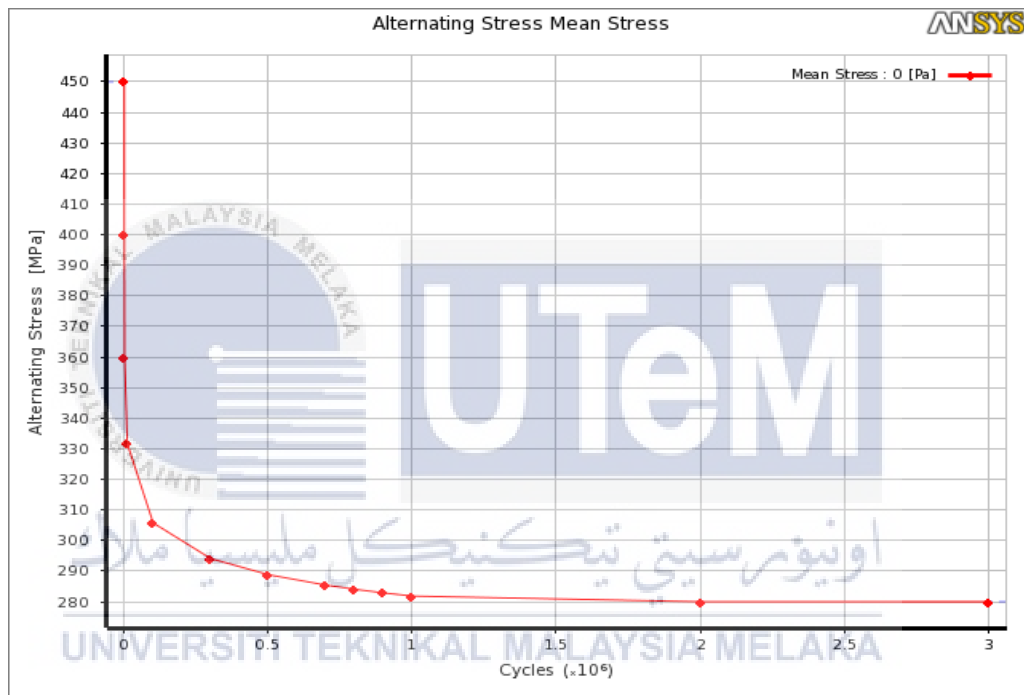


Figure 3.12: S-N curve displayed and interpolated as Linear

The alternating stress data can be used for the stress-life approach by adding this data to the engineering data as a fatigue curves. Then, fatigue tool will use the information from these curve when calculating life, damage and safety factors.

3.8.2 Mesh Generation

In this study, the creation of meshing in finite element models is the most important step in the analysis. The accuracy of result depends mainly on the meshing methods. Hence, it is essential to give more focus on the method and size meshing of the components. Basically, the automatic mesh method is generated on the mounting component. But, the elements produced by an automatic mesh generator are not well-shaped. In addition, the automatic method will show a coarse mesh which require less computational resources to solve and very inaccurate solution but this method still be used as a rough verification and as a check on the applied load and constraints.

Then, the analysis of engine mounting component were finely mesh with sizing option in outline menu. Then, element size was chosen to be 3 mm and the elastomer mount surface were refined. The meshed view of the modal is given in Figure 3.13. There are about 5161 nodes and 473300 elements to the entire geometries.

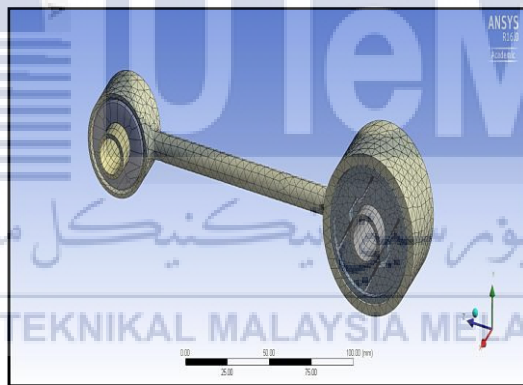


Figure 3.13: Meshed Model of Engine Mounting Component

The refinement process is a process of regenerate the model with completely better meshing compared with previous result of meshing. The several methods and changing of sizing mesh had been done in order to refine the quality of meshing. The refinement of mesh model and graph of element quality are shown in Figure 3.14. The graph shows the value element is good meshing because the graph approaching the value one. The refinement mesh of this model analysis is used only two techniques which is reducing the element size and manually adjusting the mesh. The reducing element size is the easiest strategy to overcome the unsatisfied element quality of meshing.

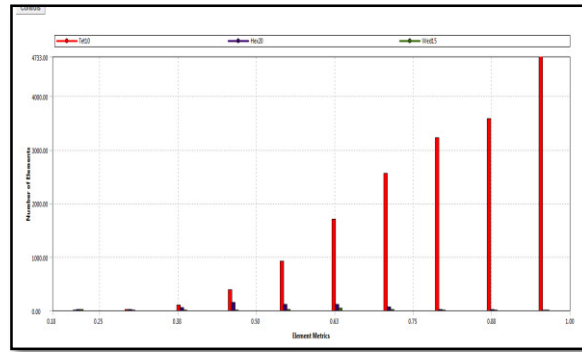


Figure 3.14: Mesh Quality Metrics Bar Graph

3.8.3 Load Condition

There are two types of loading that can be applied in this analysis which are externally applied force and temperature. The loads are used to represent inputs to the system. It can be in the forms of forces, moments, pressures, temperature etc. The contact loads are directly considered as uniformly distributed load at the inner surface as shown in Figure 3.15. The load is taken as 1500 N which is considered as the distributed weight of the engine. The load steps are considered for fatigue analysis at the small end.

اونيورسيتي تيكنيكل مليسيا ملاك
UNIVERSITI TEKNIKAL MALAYSIA MELAKA

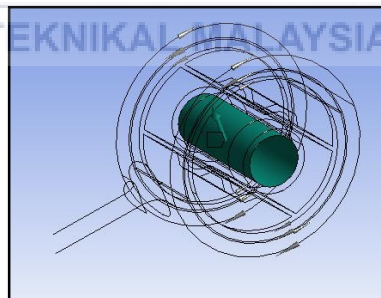


Figure 3.15: The direction of Force Applied on Component

3.8.4 Boundary Conditions

The boundary conditions are the reference points for calculating the results of analysis. Then, identification of correct boundary conditions determine the accuracy of the FE results. In this project, a rigid element is applied on the inner surface steel frame mount which assume as fixed support. The boundary loads were applied at cylindrical hole where elastomer rubber mount is bolted to the bracket. The fixed constrains view of an engine mounting component model is shown in Figure 3.16.

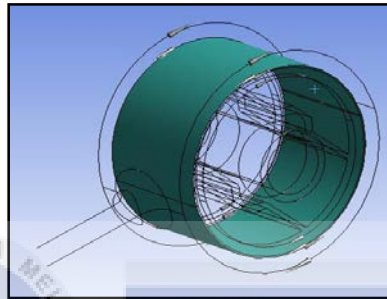


Figure 3.16: Fixed Constraints

3.8.5 Thermal Loading Condition

The thermal boundary condition for model in ANSYS is applied on the outside of the surface. The thermal condition was applied on a 3D geometry component model to make a realistic temperature condition. The elastomer part of the mounting component is focus because of the critical stress area. The thermal boundary conditions of an engine mounting component are shown in Figure 3.17. The temperature distribution (35 °C - 55 °C) is obtained from thermal inspection on an engine mounting component at actual condition. The purpose of the analysis is to predict the von-Mises stress and the fatigue life of the component when the thermal condition is applied. Basically, most engine normal operating temperature is in the range of 90 °C to 105 °C (DeLillo, 2016). But, the real consideration on temperature must include the surrounding temperature of operation for the vehicle engine. Lastly, the thermal condition is applied to provide the temperature distribution for stress analysis.

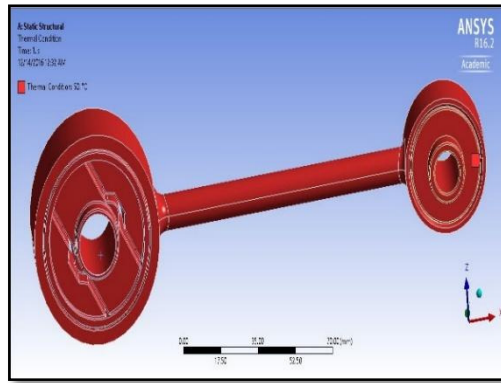


Figure 3.17: The Thermal Loading on the Component



CHAPTER 4

RESULT AND DISCUSSION

4.1 Introduction

In this chapter, the results of analysis based on the finite element method through the fatigue and thermal loading of an engine mounting component are presented. In this project, the engine mountings are modeled in CATIA software and simulation analysis using ANSYS R16 software. The results will be compared for both types of engine mounting components. From the results of the analysis, further understanding is required in determining the failure criteria for that particular component.

4.2 Mechanical Testing Experimental Work

The result of basic mechanical properties for an engine mounting component are summarized in Table 4.1. The data obtained is used to validate and set as a parameter for engineering data of FEA model for the component.

Table 4.1: Summary of Mechanical Properties of an Engine Mounting Component
Material

Property	Value
Ultimate Tensile Stress, $\sigma_{ultimate}$ (MPa)	704.18
Yield Stress, σ_{yield} (MPa)	505.43
Percent of Elongation (%)	10.7
Percent of Area of Reduction (%)	30.9
Rockwell Hardness (MPa)	9.67 / 640

The correlation value of ultimate tensile stress and yield strength are used for the verification and classification of steel. The nearby classification of steel with the experimental data is AISI/SAE 4130 steel. The correlation value of experimental data and the AISI/SAE 4130 steel are shown in Table 4.2. Furthermore, this study used the AISI/SAE 4130 steel fatigue properties to predict fatigue behavior of the engine mounting component and used as the engineering data for the finite element analysis.

Table 4.2: Mechanical Properties of AISI 4130 Steel

Material	Experimental	AISI 4130 Steel
Ultimate Tensile Stress, $\sigma_{ultimate}$ (MPa)	704.18	560 to 1040
Yield Stress, σ_{yield} (MPa)	505.43	440 to 980
Percent of Elongation (%)	10.7	25.5

Lastly, there are many factors influenced the accuracy and quality of the test results of the mechanical test which are the sample preparation, rate of load applied, metallurgy phase and the calibration of testing machine among others.

4.3 A Static Structural Analysis

A static analysis is carried out to determine the stress concentration and the total displacement on engine mounting component. The stress concentration and the displacement are carried out with both load and thermal loading condition. The results of the von-Mises stress with temperature loading effect done by ANSYS workbench software over the elastomer mount when the load pressure is 1500 N. The variation parameter of thermal loading condition are 35°C, 45°C, 55°C and 65°C assumed as the high and low temperature conditions occur at an engine mounting component. The 3D model of the Proton SAGA component shown in Figure 4.1 is taken for analysis.

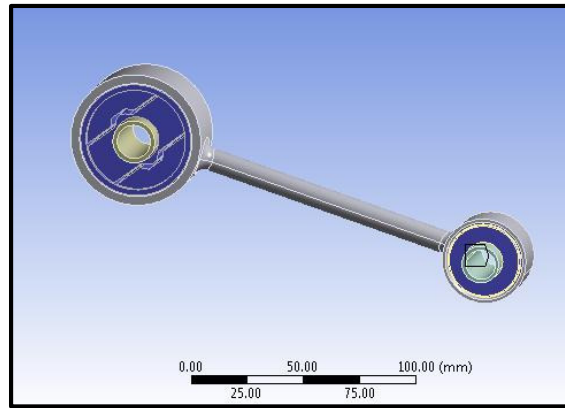


Figure 4.1: The Three Dimensional Model of the Proton SAGA Component

Based on the result of mechanical testing on the engine mounting component, it shows the data was closely reflected the properties of AISI/SAE 4130 steel. Therefore, the existing model of an engine mounting component consist of AISI/SAE 4130 Steel and Elastomer (Butyl Rubber) as material of the component. AISI/SAE 4130 and Butyl Rubber are mainly used in automotive application due to the lightweight, high strength and high temperature application. The material properties used for the engineering data ANSYS R16 are listed in Table 4.3.

Table 4.3: The Engineering Data for the Simulation in ANSYS R16 Workbench

Properties	AISI/SAE 4130 Steel	Elastomer (Butyl Rubber)
Young's Modulus, E (GPa)	210	0.0015
Poisson Ratio, ν	0.29	0.3
Yield Stress, σ_{yield} (MPa)	505	2.5
Ultimate Tensile Stress, σ_{ultimate} (MPa)	704	7.5
Density, ρ (g/m^3)	7.85	0.91×10^6

References:

Properties of AISI/SAE 4130 Steel – (Jeelani, 2016)

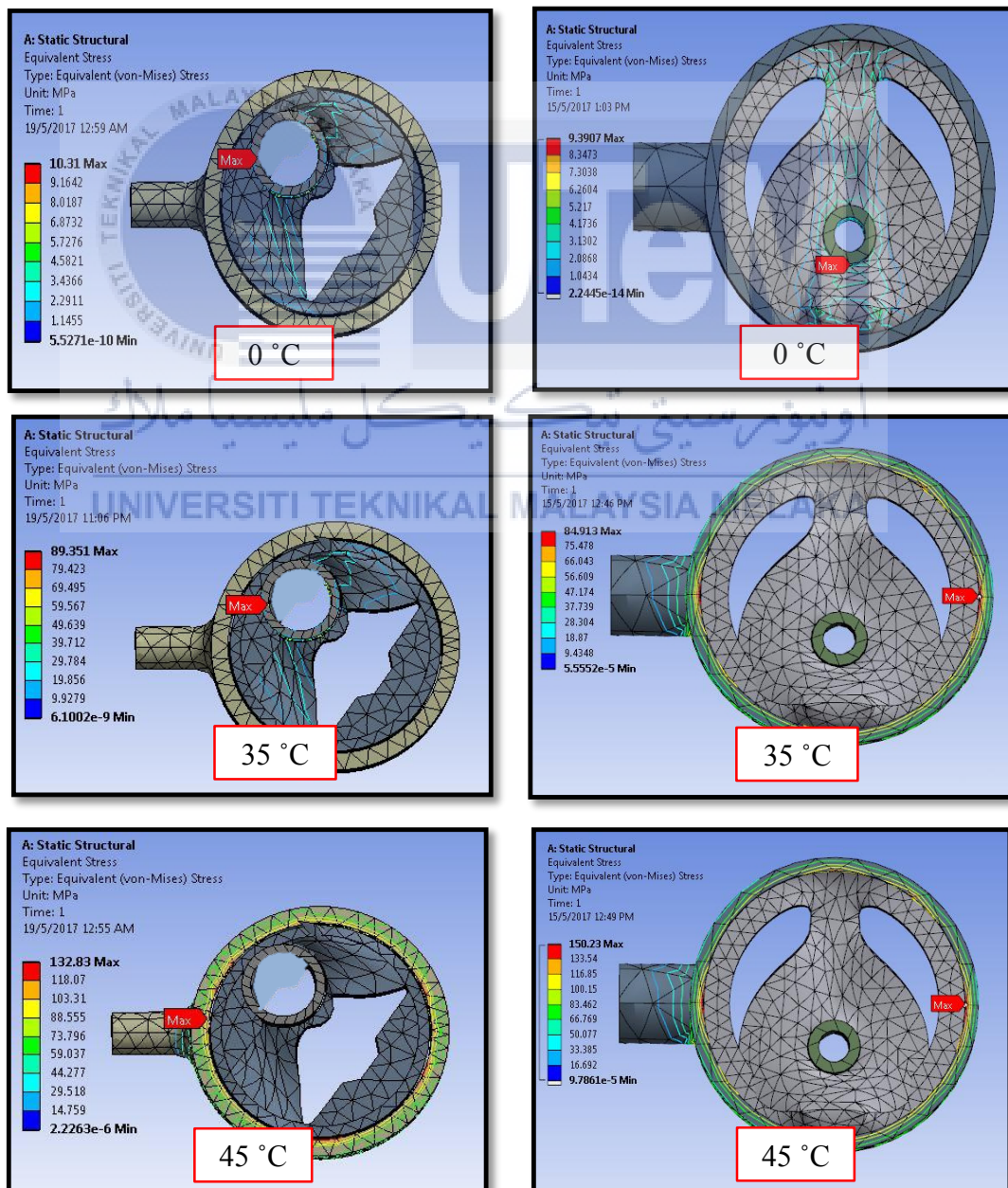
Properties of Elastomer (Butyl Rubber) Material - (M F Ashby, 2003)

4.3.1 The Von-Mises Stress Analysis on the Elastomer with Thermal Effect

Static von-Mises stress analysis was carried out for engine mounting component. The result of von-Mises stress with temperature loading effect done by ANSYS workbench software over the elastomer mount part when applied force is 1500 N. This force is taken into consideration of the average weight of distribution of engine. The corresponding elastomer mount temperatures are 35°C, 45°C, 55°C and 65°C respectively. The results for von-Mises stress of the engine mounting component is shown in Table 4.4 and the contour plots of von-Mises stresses are shown in Figure 4.2.

PROTON SAGA

PERODUA KANCIL



PROTON SAGA

PERODUA KANCIL

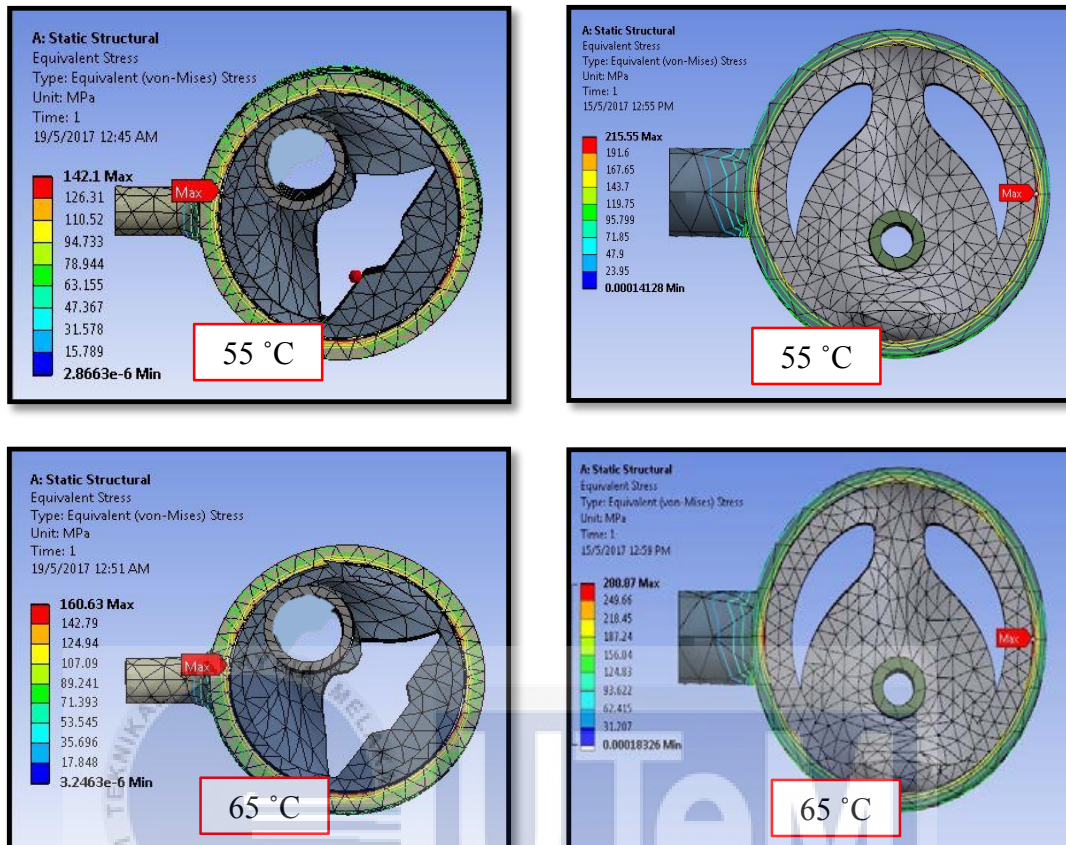


Figure 4.2: Maximum Stress of Elastomer Mount at Different Temperature

From the Figure 4.2, the contour plot of von-Mises stress is indicated by the red color which has the maximum value and minimum value is indicated by blue color. Also the figure depicted that the von-Mises stress is high at around edge frame mount in contact with the elastomer mount of the component. The results are shown in Table 4.4 and the graph plotted for the maximum value of the von-Mises proportional to temperature change as shown in Figure 4.3.

Table 4.4: The Results Von Mises Stress with Thermal Loading

Temperature	Proton SAGA	Perodua KANCIL
0 °C	10.31 MPa	9.39 MPa
35 °C	89.35 MPa	84.9 MPa
45 °C	132.82 MPa	150.2 MPa
55 °C	142.1 MPa	215.6 MPa
65 °C	160.63 MPa	280.9 MPa

Von-Mises Stresses Vs Different Temperature

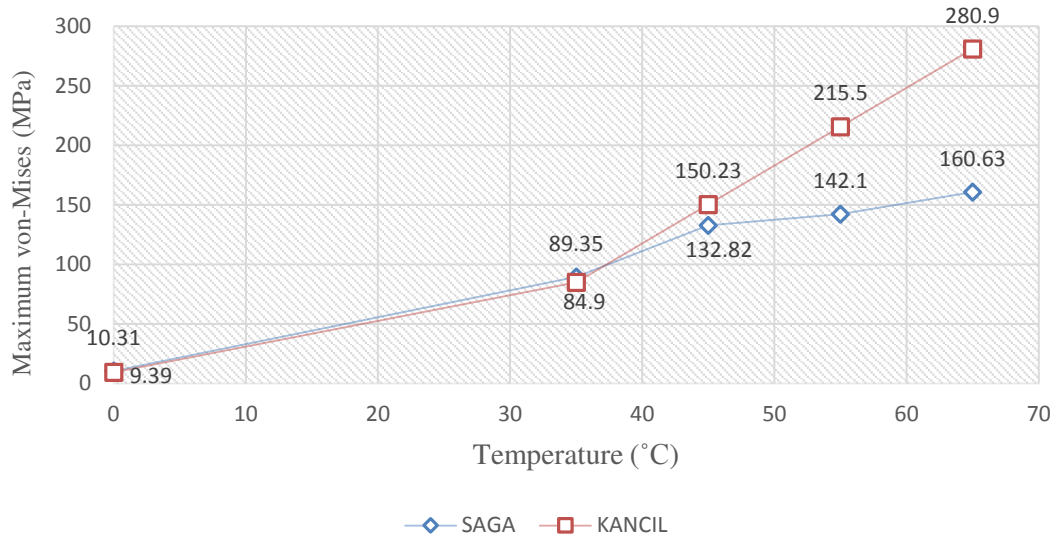


Figure 4.3: Graph of von-Mises Stresses with Thermal Loading

It was found that the higher temperature applied on the mount component, the value of stress of the elastomer part is also higher. This is because of the thermal effect on the properties of the material changed especially on the elastomer part. Then, the Perodua KANCIL mount shows that highest value of the stress compare to the Proton SAGA mounting component. The maximum critical area of stress concentration region is located on the inner frame of the component. The critical area indicated at same location on the both type of the component. The Figure 4.4 and Figure 4.5 show the critical stress region on the elastomer part for both type. The improvement of the design for an engine mounting component must be focused at the rubber and metal bonding assembly.

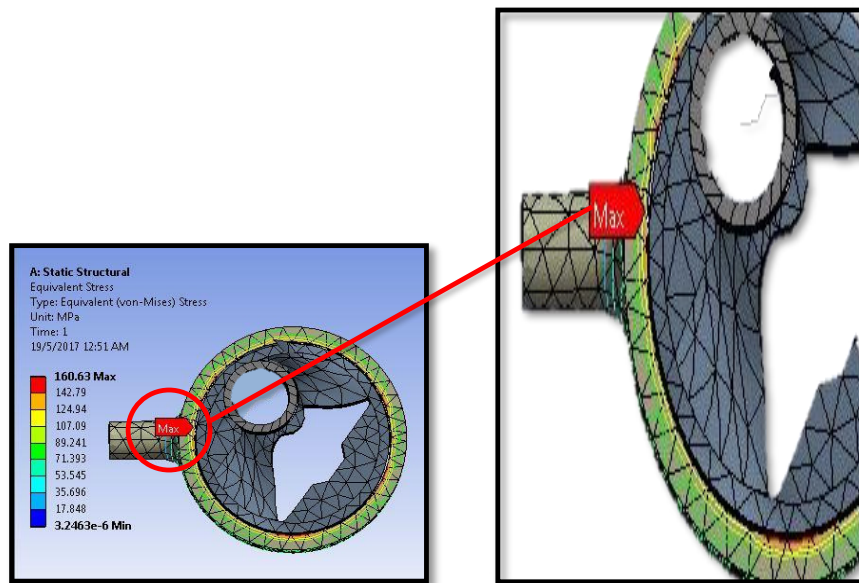


Figure 4.4: The Maximum Stress Region on the Proton SAGA Component

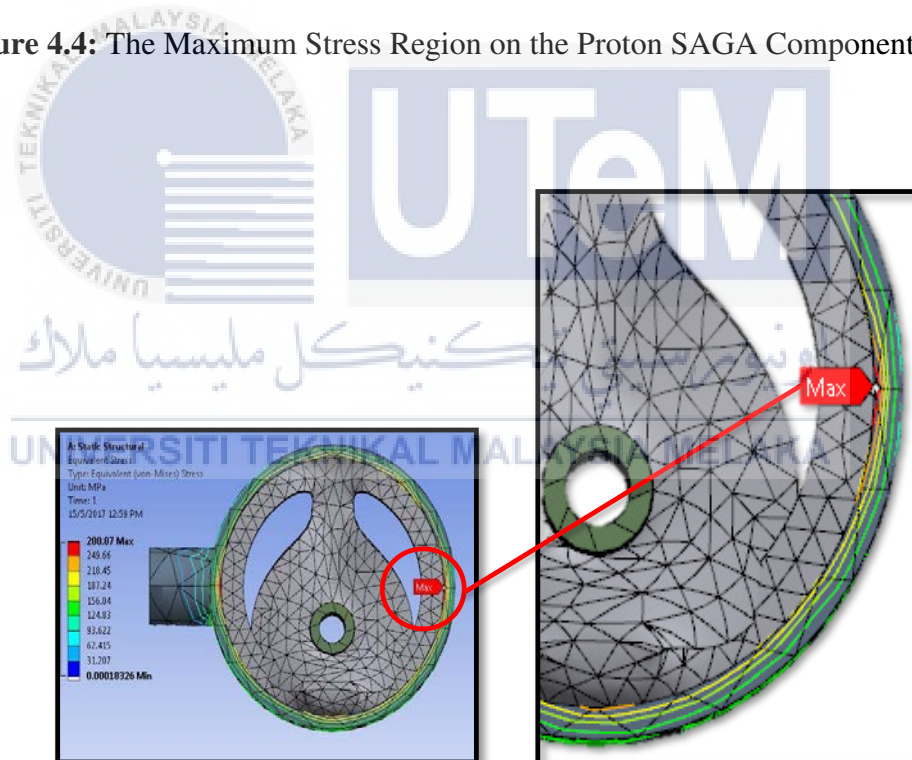


Figure 4.5: The Maximum Stress Region on the Perodua KANCIL Component

4.3.2 Total Deformation and Factor of Safety with Thermal Loading Effect on the Elastomer

The result of total deformation with the maximum temperature loading effect done by ANSYS R16 workbench software over the elastomer mount part when the applied force is 1500 N. The maximum total deformation was found to be 28.09 mm for the Proton SAGA component and the 32.37 mm for the Perodua KANCIL component. Figure 4.6 shows the contour plot with the maximum total deformation occurred is around the bolt's hole of the elastomer mount part.

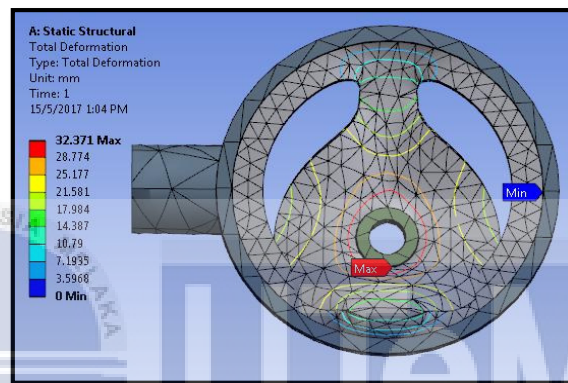


Figure 4.6: The Maximum Total Deformation of Elastomer Mount (Perodua KANCIL Component)

The specification of the elastomer part is shown in Table 4.5. It shows that the volume of the Perodua KANCIL is 32556 mm³ compared to the Proton SAGA component is 40185 mm³. Then, the diameter of elastomer on Perodua KANCIL is 52 mm compared to 57 mm for the Proton SAGA. The total deformation is high on the Perodua KANCIL because of the diameter and width are smaller compared to Proton SAGA. The result of the total deformation is influenced by the diameter and width of component.

Table 4.5: The Specification of the Elastomer Part

Specification	Proton SAGA	Perodua KANCIL
Volume (mm ³)	40185	32556
Diameter (mm)	57	52
Width (mm)	28	24
Total Deformation (mm)	28.09	32.37

Moreover, the analysis for maximum factor of safety was found equal to 15 for both of the components. However, the minimum factor of safety (SF) was found of 0.76 on Proton SAGA and 0.3 on the Perodua KANCIL respectively. The findings show that there will be a failure on the area around the rubber and metal bonding. The flaw can easily produce at the critical region of the component due the design weakness. The results of FS were obtained based on the theory of the von Mises failure criterion. The theory states that a ductile material start yielding at a location when the von Mises stress becomes equal to the stress limit. Figure 4.7 shows contour plot of the maximum and minimum values of the factor of safety, the value is indicated based on the maximum critical region and the minimum stress region at the elastomer part. According to the von Mises failure criterion the factor of safety (FS) is expressed as equation 4.1. Lastly, the FEA simulation is used to evaluate the factor of safety at the part only not the whole of the component, in the study the elastomer part is selected because the failure occur at this part. The FS also defined as the ratio between the strength of the material and the maximum stress in the part.

$$\text{Safety Factor (SF)} = \frac{\sigma_{\text{yield limit}}}{\sigma_{w(\text{allowable})}} \quad (4.1)$$

$$\text{Safety Factor (SF)} = \frac{2.5 \text{ MPa}}{0.1669 \text{ MPa}} = 14.97$$

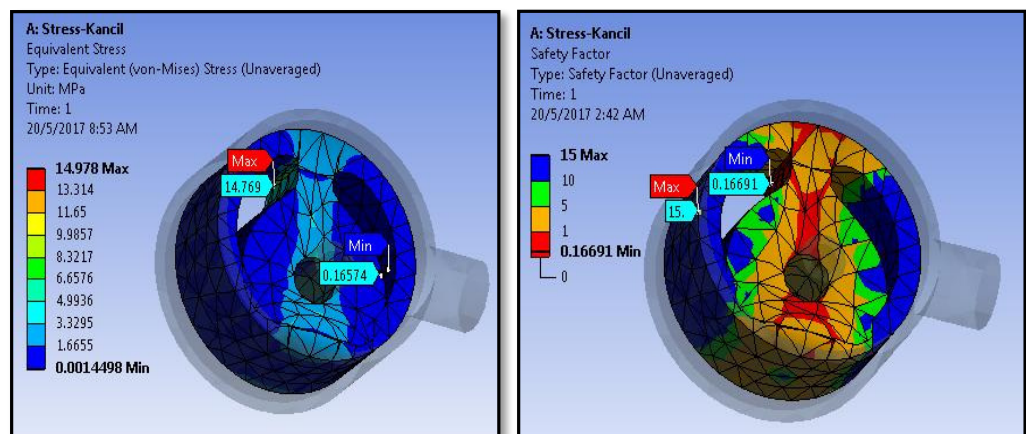


Figure 4.7: The Safety Factor of Elastomer Mount
(Perodua KANCIL Component)

4.3.3 Fatigue Analysis with Thermal Loading Effect of Steel Part

The fatigue analysis is carried out to determine the fatigue behavior of the component under maximum thermal loading. The Von-Mises stress are imported to the fatigue analysis and results are obtained. The force applied on the inner bolts hole of engine mounting component is 1500 N. This method is developed on the finite element analysis in order to predict the fatigue life of the engine mounting component. The fatigue tool used the information from the S-N curve for the AISI/SAE 4130 steel material. However, the ultimate tensile stress and yield stress based on the result of tensile test was used for the FEA. The alternating stress data are listed in Table 4.6.

Table 4.6: Properties of Fatigue Modification

Fatigue Tool

Property	Value
Interpolation	Log-Log
Scale	1
Curve Type	Stress-Life
Cyclic Strength Coefficient	1000 MPa
Cyclic Strain Hardening Exponent	0.2
Fatigue Strength Factor	1.0
Type	Fully Reversed
Scale Factor	1.0

An ANSYS R16 workbench on the fatigue tool used the graphical cyclic stress on the analysis. This also clear from the Goodman Model where the S-N curve is used to define fatigue life. The graphical representation of the S-N curve data is shown in Figure 4.8 for the steel component. The alternating stress (S_n) is reducing with number of cycles (N). Then, fatigue limit corresponding to one million cycles represented by 136.58 MPa for the material. So, fatigue analysis is carried out for this endurance limit with the high cycle region is considered. Moreover, fatigue life is specified for one million cycles which is defined with endurance limit of the material under reversed loading.

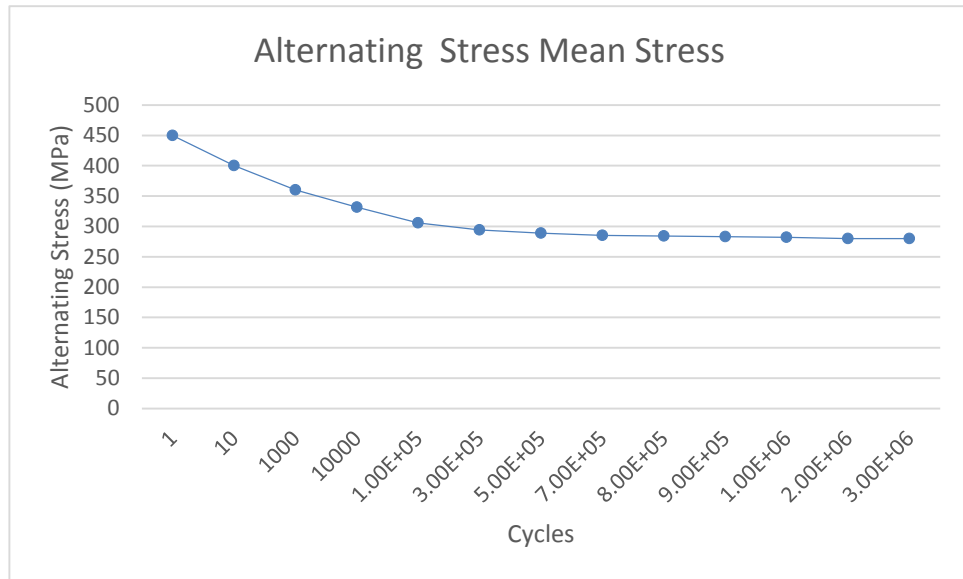


Figure 4.8: S-N Curve Displayed and Interpolated as Linear

The fatigue performance can be calculated from the relations between fatigue and tensile properties of the material. The ratio of the endurance limit (S_e) to the ultimate strength (S_u) of a material is called the fatigue ratio. For steel, the endurance strength can be approximated by calculation and equations 4.2 – 4.6 are used;

Stress Amplitude:

$$\sigma_a = \frac{\sigma_{max} - \sigma_{min}}{2} \quad (4.2)$$

$$\sigma_a = \frac{600 - 120}{2} = 240 MPa$$

Mean Stress:

$$\sigma_m = \frac{\sigma_{max} + \sigma_{min}}{2} \quad (4.3)$$

$$\sigma_m = \frac{600 + 120}{2}$$

$$\sigma_m = 360 MPa$$

Goodman Model equation is given by:

$$\frac{\sigma_a}{\sigma_n} + \frac{\sigma_m}{\sigma_u} = 1 \quad (4.4)$$

$$\frac{240}{\sigma_n} + \frac{360}{704} = 1$$

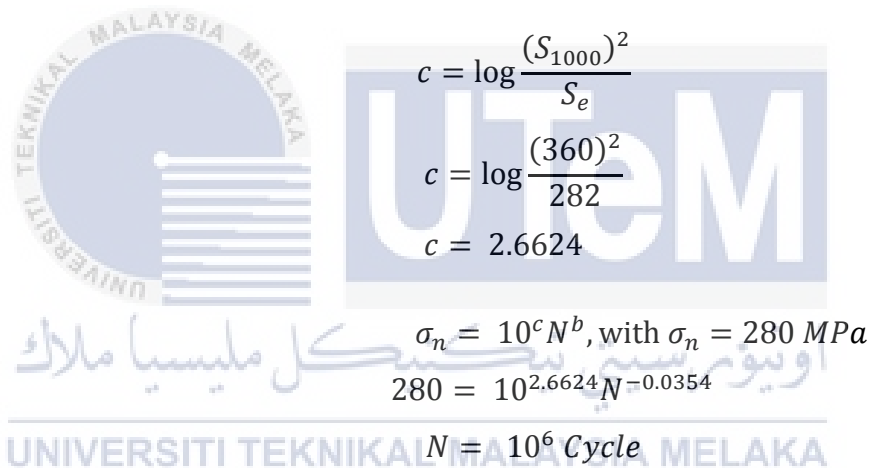
$$\sigma_n = 490.0 MPa$$

The fatigue limit of steel with ultimate tensile strength below 1400 MPa is estimated as follows;

$$\begin{aligned} S_e, \text{ steel} &\approx 0.4 \text{ for } S_{ult} < 1400 \text{ MPa} && (4.5) \\ &= 0.4 \times 704 \text{ MPa} \\ &= 282 \text{ MPa} \end{aligned}$$

$$\text{Linear S-N equation: } \sigma_n = 10^c N^b \quad (4.6)$$

$$\begin{aligned} b &= -\frac{1}{3} \log \frac{S_{1000}}{S_e} \\ b &= -\frac{1}{3} \log \frac{360}{282} \\ b &= -0.0354 \end{aligned}$$



$$\begin{aligned} c &= \log \frac{(S_{1000})^2}{S_e} \\ c &= \log \frac{(360)^2}{282} \\ c &= 2.6624 \end{aligned}$$

$$\begin{aligned} \sigma_n &= 10^c N^b, \text{ with } \sigma_n = 280 \text{ MPa} \\ 280 &= 10^{2.6624} N^{-0.0354} \\ N &= 10^6 \text{ Cycle} \end{aligned}$$

The alternating stress from 1 cycles to 3 million cycles used to construct the stress-life curve that represents fatigue data. These data are often fit to a simple power function relating stress amplitude to fatigue life. The alternating stress developed is around 280 MPa which is less than the fatigue limit is 283 MPa for one million cycles ($N = 10^6$ cycles) as listed in Table 4.7.

Table 4.7: S-N Curve Displayed and Interpolated As Linear

Cycles	Alternating Stress (MPa)
1	400
10	450
1000	359.92
10000	331.74
1E+05	305.77
3E+05	294.11
5E+05	288.84
7E+05	285.42
8E+05	284.07
9E+05	282.89
1E+06	281.84
2E+06	280
3E+06	280

The data of the alternating stress can be used for the Stress-life approach by adding this data to the engineering data as a fatigue curves. Then, fatigue tool will use the information from this curve to calculate fatigue life and factor of safety (FS). A finite element analysis (FEA) is carried out at local region at high stress under operating condition. The cyclic loading applied on component will result in equivalent alternating stress.

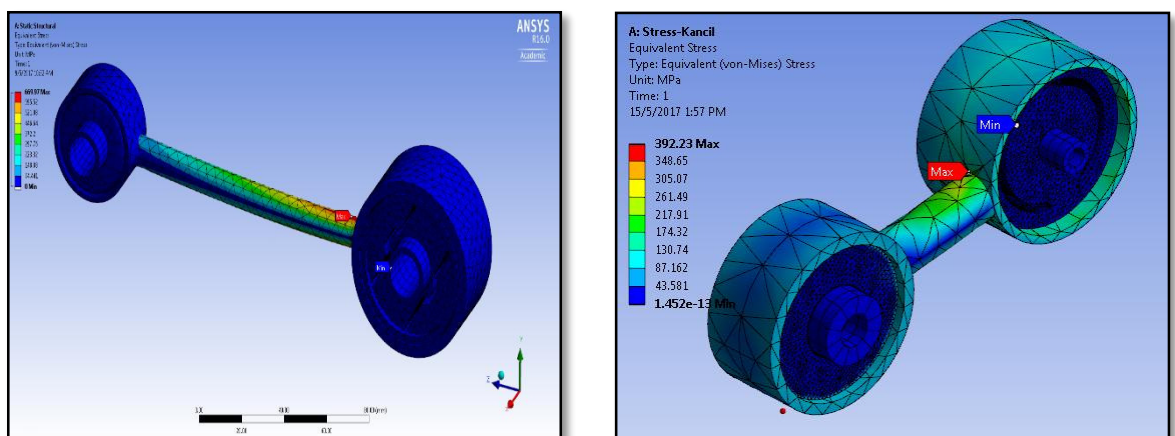


Figure 4.9: Contour Plot of Equivalent Alternating Stress of the Component

The result of the fatigue analysis is shown in the form of equivalent alternating stress with the variation temperature loading effect done by ANSYS R16 over the steel part where the applied force is 1500 N. In this study, it is found that the maximum equivalent alternating stress is 669.89 MPa for the Proton SAGA component and 430.13 MPa for Perodua KANCIL component at 65 °C as shown in Figure 4.9. The results are listed in Table 4.8 for the maximum equivalent alternating stress with the different temperature.

Table 4.8: The Results Equivalent Alternating Stress with Thermal Loading

Temperature	Proton SAGA	Perodua KANCIL
0 °C	345.65	286.14
35 °C	435.87	323.37
45 °C	542.01	356.41
55 °C	586.43	392.23
65 °C	669.89	430.13

The curve presented in Figure 4.10 shows the result of fatigue equivalent alternating stress at the structure mount frame due the variation of thermal loading. It is noticed that the von-Mises stress increase with the increasing of temperature applied on the component. The curve also shows that the SAGA component is expected to have higher stresses compare to the KANCIL component. Highest stress can be observed at the connecting joint rod region and almost the minimum stress at the bolt assemble hole. It is because the size of the connecting rod of Proton SAGA is 10 mm diameter and the length is 115 mm as tabulate in Table 4.9. This shows the SAGA has a smaller geometry compared to the KANCIL component. Another factor of the high stress concentration also attributed to the weld at end of connecting rod. The stress concentration can significantly effect the fatigue life of the component.

Table 4.9: The Size of Connecting Rod

Specification	Proton SAGA	Perodua KANCIL
Diameter (mm)	10	15
Length (mm)	115	36

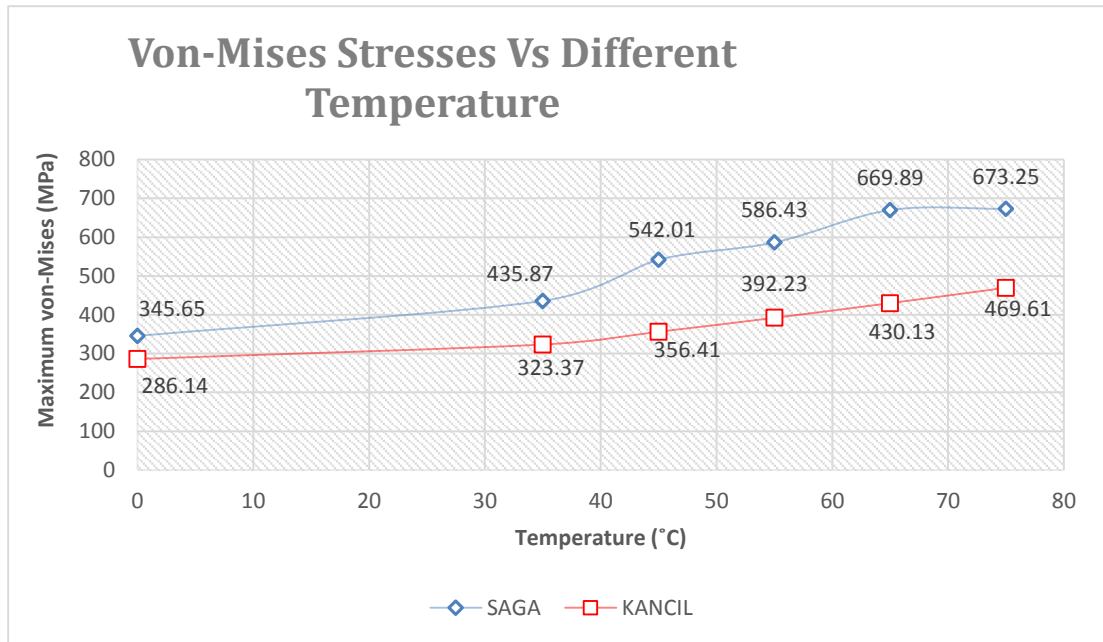


Figure 4.10: Graph of Fatigue Equivalent Alternating Stress with Thermal Loading

The fatigue life of the component is typically localized at points of high stress on the connecting rod. Then, a cycle counting method procedure relates the damage effect of constant amplitude.

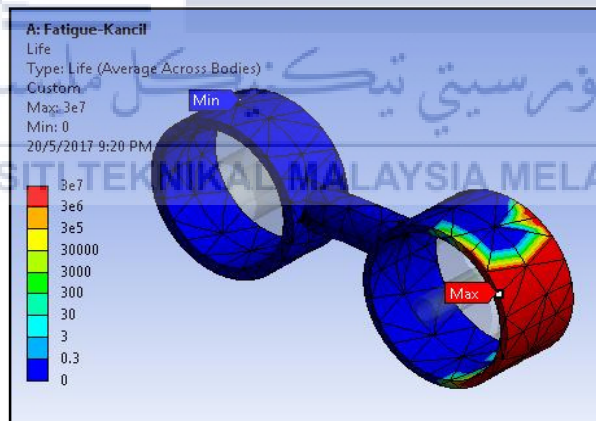


Figure 4.11: The Fatigue Life of Elastomer Mount Perodua KANCIL

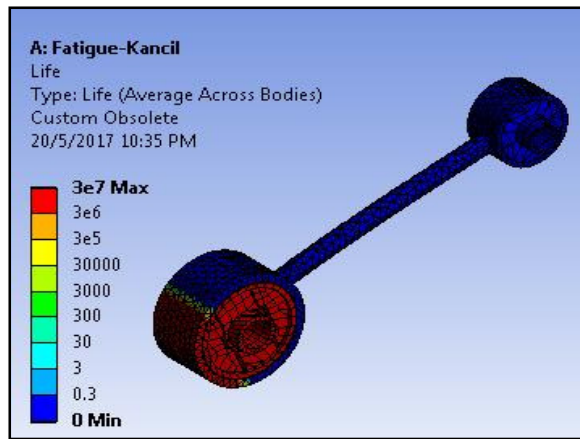


Figure 4.12: The Fatigue Life of Elastomer Mount Proton SAGA

The life of the steel frame component obtained 10^6 cycles as shown in contour results are shown in Figures 4.11 and 4.12 respectively. The maximum temperature and fatigue loading was used to determine fatigue limit. The simulation result shown above, 3×10^6 cycles is the expected life of the component due to the applied force and maximum thermal loading condition. In this study the availability of details data of fatigue behavior for the engine mounting component is limited because there are no manufacturing company published such data. Even through this mount component has their own advantages and function ability compare to the new technology of engine mount component that increasing over the years. This analysis data can be used further for the mechanical fatigue with thermal effect analysis and fail-safe design method in the future.

CHAPTER 5

CONCLUSION AND RECOMMENDATION

5.1 Conclusion

In this study, cyclic stresses and thermal loading is presented for the finite element method of an engine mounting component. The method developed in this study can be used to analyze the behavior of the elastomer mount and the whole component. The Proton SAGA and Perodua KANCIL mounting components have been compared by using ANSYS workbench analysis results, where it can be used to predict fatigue life, design optimization and defining of safety factor either with or without thermal effects. Generally; based on this study the following conclusion may be made:

- 1) The material properties and fatigue life evaluation of steel and rubber are very important in design procedure to assure the safety and reliability of the engine mounting components.
- 2) The results obtained from the static structural analysis shows that the maximum critical area of stress concentration region is located on the inner frame and bolts hole of the component. The improvement of the design must be focused at the rubber and metal bonding assembly.
- 3) In this study the thermal loading effect influenced the result of alternating stress of the component. The result obtained from the analysis indicates that the higher temperature loading applied on the component, will lead to a higher of alternating stress of the component.
- 4) The fatigue resistance of the steel could be conservatively predicted by the experimental development using fatigue design curves for normal strength steel. This would be beneficial to both the steel and automotive industries to understand how mechanical properties correlate with fatigue performance across

a wide range of engine mounting components since fatigue tests are very time consuming and expensive.

- 5) The analysis on the fatigue life of engine mounting components play an important role in the design, safety and reliability of vehicles.

5.2 Recommendation

The following recommendations are given in order to improve the present study and should be taken into consideration in future work:

- 1) For the elastomer mount of the component within cyclic stresses and thermal loading effect, it would be interesting to conduct experimental study to validate the results of ANSYS workbench software.
- 2) The study carried out provided an evaluation of the stress life approach in predicting fatigue life of the real engine mounting component. However, there are significant areas that require further investigation and evaluation especially in the field of fatigue life behavior of elastomer.
- 3) Since determining the fatigue performance of engine mounting components extremely difficult due to the different stress combinations and different environmental circumstances, the effects of these damage sources on the fatigue performance needs further study and to be included in simulation works.
- 4) Predicting the fatigue life of a metal part is complicated because materials are sensitive to small changes in loading conditions and the stress concentrations and other factors. All these conditions need to be considered in future work.
- 5) Explore with different type of finite element analysis (FEA) software to predict durability and fatigue life with nonlinear behavior of elastomer part on the engine mounting component. Example, the Endurica CL simulation software with a full featured solver providing elastomer fatigue analysis.

REFERENCES

- A.Agharkakli,D. P. Wagh. (2013). Linear Characterization of Engine Mount and Body Mount for Crash Analysis. International Journal of Engineering and Advanced Technology, 2249 – 8958.
- ASME-E8. (2003). Standard Test Methods for Tension Testing of Metallic Materials. An American National Standard, 3.
- ASTM_E-18. (2012). Standard Test Methods for Rockwell Hardness of Metallic Materials. ASTM E-18, 36.
- Bobbili, R. (2015). Tensile Behaviour of Aluminium 7017 Alloy. Journal of Materials Research and Technology, 5.
- Chawla, S. L. (1993). Material Selection for Corrosion Control. Delhi: ASM International.
- DeLillo, J. (2016, October 1). Should I Worry About How Hot My Engine Is Running? Retrieved from cars.com: <https://www.cars.com/articles/should-i-worry-about-how-hot-my-engine-is-running-1420680334271/>
- Devarasiddappa, D. (2006). Automotive Applications of Welding Technology. International Journal Of Modern Engineering Research (IJMER), 1.
- G.S. Cole, A. S. (1995). Light weight materials for automotive applications. In Materials Characterization (pp. 3-9).
- Gliner, B. (1960). The Mechanical Testing of Metals. Determination of the Mechanical and Technological Properties of Metals, 56.
- Hagino, Y. (1991). An Analysis and Application of a Decoupled Engine Mount System. Vibration and Control.
- Heisler, H. (2002). Advance Vehicle Technology. Butterworth: Heinemann.
- J.Bretl. (1993). Optimization of Engine Mounting Systems to Minimize Vehicle Vibration. SAE Papers.
- J.C.Snowdon. (1968). Vibration and Shock in Damped Mechanical Systems. Wiley.
- Jadav Chetan, P. K. (2012). A Review of the Fatigue Analysis of An Automotive Frame. International Journal of Fatigue, 3.

- Jeelani, S. (2016, March 14). Fatigue For 4130 Steel. Retrieved from MSState Education: https://icme.hpc.msstate.edu/mediawiki/index.php/Fatiguelife_
- Krzysztof Kluger, T. L. (2013). Fatigue Life of Metallic Material Estimated According to Selected Model and Load Conditions. *Journal of Theoretical and Applied Mechanics*, 581-592.
- Kumar, K. (2008). Academia. Retrieved from Finite Element Analysis Notes On One Dimensional Structural Analysis: https://www.academia.edu/8224942/FINITE_ELEMENT_ANALYSIS_NOTES_ON_ONE_DIMENSIONAL_STRUCTURAL_ANALYSIS
- M F Ashby, D. R. (2003). *Material Data Book*. Cambridge University Engineering Department.
- M. R Ayatollahi, F. M. (2011). Thermo-Mechanical Fatigue Life Assessment of a Diesel Engine Piston. *International Fatigue Journal*, 258.
- M.S. Loveday, R. M. (1998). Standard of Mechanical Testing and Quality Control. *High Technology Metal*, 103-122.
- Meyer, M. (1989). A Theory of Rockwell Ball Hardness. *Laboratorium*, 11-26.
- Michael Champrenault, C. A. (2007). New Application of Material Being used in this Sub-System for Vehicle Mass Reduction. *Magnesium Power Train Mount Bracket*, 1.
- Miller, L. (1992). Active Mounts of Future Technology Trends. *Inter-Noise Conference Toronto*, (pp. 1-6). Canada.
- P.E Geck, R. P. (1992). Front Wheel Drive Engine Mount Optimization. *Ohio State University*, 47-57.
- Philipfigari. (2008). Autodesk Corporation. Retrieved from Autodesk Inc: <https://www.instructables.com/id/Steps-to-Analyzing-a-Materials-Properties-from-its/>
- Qasim, B. (2014). Mean Stress Correction Effects On the Fatigue Life Behaviour of Steel. *International Journal of Engineering & Technology*, 2.
- R.C, H. (2008). *Structural Analysis*. U.K: Pearson Education.
- Ramamurty, G. (2010). *Applied Finite Element Analysis*. India: L.K International Publishing House Pvt.Ltd.
- Rubber metal bonding - Bond system characteristics. (2003). Retrieved from Processing of Rubber Materials: https://www.tut.fi/ms/muo/vert/8_processing/4.7.b.htm
- S.H. Lee, Y.S Lim. (2006). The Development and Performance Simulation of Polychloroprene High Temperature Bush Type Engine Mounting . *SAE Journal*.

- S.Koushik. (2013). Static and Vibration Analysis of Engine Mounting Bracket of TMX 20-2 using Opti Struct. Altair Technology Conference.
- Thomas, A. (1958). Rupture of Rubber. Part V. Cut Growth In Natural Rubber. Journal of Polymer Science, 467.
- Tushar Tandon, N. K. (2015). Stress Analysis of Costal RADAR antenna Mounting Base using ANSYS. Material Processing and Characterization, 2247.
- Y. Naganathan, D. (2001). Literature Review of Automotive Vehicle Engine Mounting System. Mechanism and Machine Journal, 123-142.
- Zhang Yunxia, Z. J. (2008). Modeling and Experimental. Chinese Journal of Mechanical Engineering, 1.
- Zhi-Wei Yu, X.-L. X. (2015). Fatigue Fracture of Truck Diesel Engine Connecting Rods. Journal of Failure Analysis and Prevention, 311-319.



LIST OF APPENDIX

APPENDIX TITLE

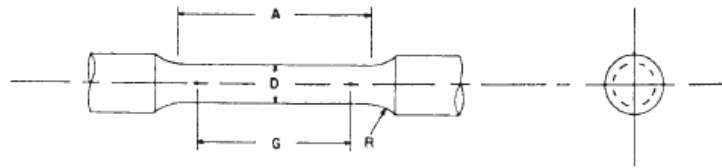
- | | |
|---|--|
| A | ASTM E-08 Metallic Tensile Test Standard |
| B | Technical Drawing – Specimen for Tensile Test |
| C | Result of Tensile Test Specimen |
| D | Sample Calculation for Tensile Test |
| E | Hardness Conversion Table |
| F | Technical Drawing – Proton SAGA Engine Mounting |
| G | Technical Drawing – Perodua KANCIL Engine Mounting |
| H | Gantt Chart of PSM I and PSM II |

اونيورسيتي تيكنيكل مليسيا ملاك

UNIVERSITI TEKNIKAL MALAYSIA MELAKA

APPENDIX A: ASTM-E8 for the Tensile Testing

E 8 - 04



Nominal Diameter	Dimensions				
	Standard Specimen		Small-Size Specimens Proportional to Standard		
	in.	in.	in.	in.	in.
	0.500	0.350	0.250	0.160	0.113
G—Gage length	2.000 ± 0.005	1.400 ± 0.005	1.000 ± 0.005	0.640 ± 0.005	0.450 ± 0.005
D—Diameter (Note 1)	0.500 ± 0.010	0.350 ± 0.007	0.250 ± 0.005	0.160 ± 0.003	0.113 ± 0.002
R—Radius of fillet, min	3/8	1/4	3/16	5/32	3/32
A—Length of reduced section, min (Note 2)	2 1/4	1 3/4	1 1/4	3/4	5/8

NOTE 1—The reduced section may have a gradual taper from the ends toward the center, with the ends not more than 1 % larger in diameter than the center (controlling dimension).

NOTE 2—If desired, the length of the reduced section may be increased to accommodate an extensometer of any convenient gage length. Reference marks for the measurement of elongation should, nevertheless, be spaced at the indicated gage length.

NOTE 3—The gage length and fillets may be as shown, but the ends may be of any form to fit the holders of the testing machine in such a way that the load shall be axial (see Fig. 9). If the ends are to be held in wedge grips it is desirable, if possible, to make the length of the grip section great enough to allow the specimen to extend into the grips a distance equal to two thirds or more of the length of the grips.

NOTE 4—On the round specimens in Figs. 8 and 9, the gage lengths are equal to four times the nominal diameter. In some product specifications other specimens may be provided for, but unless the 4-to-1 ratio is maintained within dimensional tolerances, the elongation values may not be comparable with those obtained from the standard test specimen.

NOTE 5—The use of specimens smaller than 0.250-in. diameter shall be restricted to cases when the material to be tested is of insufficient size to obtain larger specimens or when all parties agree to their use for acceptance testing. Smaller specimens require suitable equipment and greater skill in both machining and testing.

NOTE 6—Five sizes of specimens often used have diameters of approximately 0.505, 0.357, 0.252, 0.160, and 0.113 in., the reason being to permit easy calculations of stress from loads, since the corresponding cross-sectional areas are equal or close to 0.200, 0.100, 0.0500, 0.0200, and 0.0100 in.², respectively. Thus, when the actual diameters agree with these values, the stresses (or strengths) may be computed using the simple multiplying factors 5, 10, 20, 50, and 100, respectively. (The metric equivalents of these five diameters do not result in correspondingly convenient cross-sectional areas and multiplying factors.)

FIG. 8 Standard 0.500-in. Round Tension Test Specimen with 2-in. Gage Length and Examples of Small-Size Specimens Proportional to the Standard Specimen

6.5.1 For material with a nominal thickness of 0.0005-0.1875 in., use the sheet-type specimen described in 6.3.

6.5.2 For material with a nominal thickness of 0.1875-0.500 in., use either the sheet-type specimen of 6.3 or the plate-type specimen of 6.2.

6.5.3 For material with a nominal thickness of 0.500-0.750 in., use either the sheet-type specimen of 6.3, the plate-type specimen of 6.2, or the largest practical size of round specimen described in 6.4.

6.5.4 For material with a nominal thickness of 0.750 in., or greater, use the plate-type specimen of paragraph 6.2 or the largest practical size of round specimen described in 6.4.

6.5.4.1 If the product specifications permit, material of a thickness of 0.750 in., or greater may be tested using a modified sheet-type specimen conforming to the configuration shown by Fig. 2. The thickness of this modified specimen must be machined to 0.400 +/- 0.020 in., and must be uniform within 0.004 in. throughout the reduced section. In the event of disagreement, a round specimen shall be used as the referee specimen.

6.6 Specimens for Wire, Rod, and Bar:

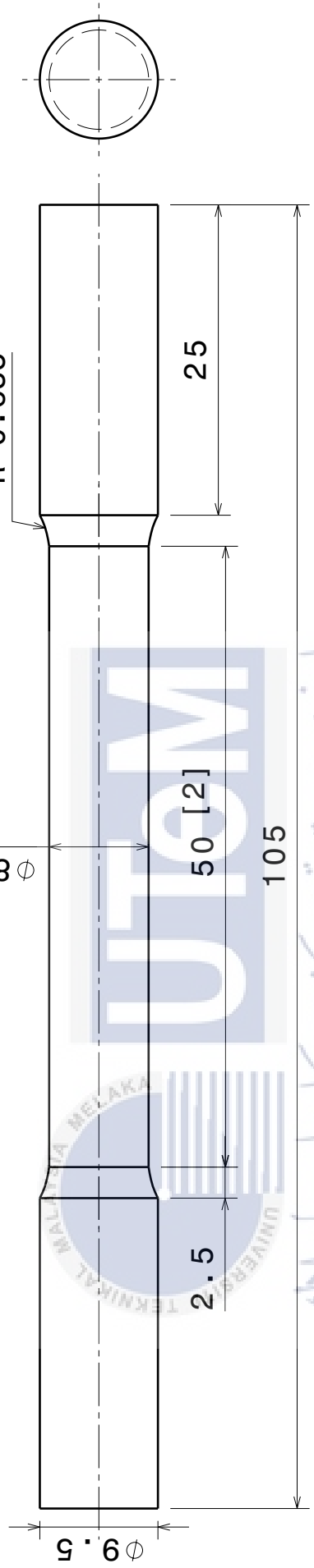
6.6.1 For round wire, rod, and bar, test specimens having the full cross-sectional area of the wire, rod, or bar shall be used wherever practicable. The gage length for the measurement of elongation of wire less than 1/8 in. in diameter shall be as

prescribed in product specifications. In testing wire, rod, or bar that has a 1/8-in. or larger diameter, unless otherwise specified, a gage length equal to four times the diameter shall be used. The total length of the specimens shall be at least equal to the gage length plus the length of material required for the full use of the grips employed.

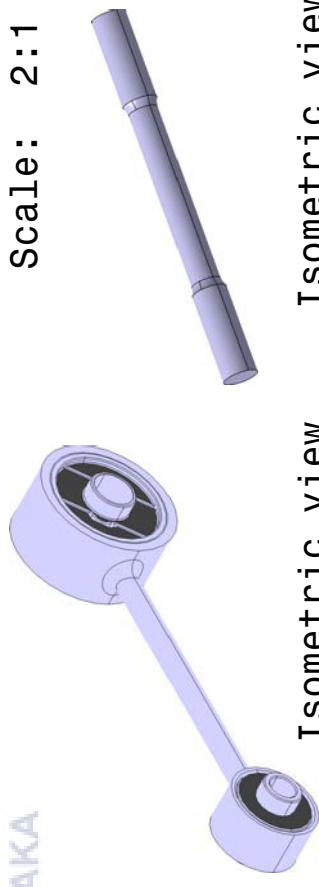
6.6.2 For wire of octagonal, hexagonal, or square cross section, for rod or bar of round cross section where the specimen required in 6.6.1 is not practicable, and for rod or bar of octagonal, hexagonal, or square cross section, one of the following types of specimens shall be used:

6.6.2.1 *Full Cross Section* (Note 10)—It is permissible to reduce the test section slightly with abrasive cloth or paper, or machine it sufficiently to ensure fracture within the gage marks. For material not exceeding 0.188 in. in diameter or distance between flats, the cross-sectional area may be reduced to not less than 90 % of the original area without changing the shape of the cross section. For material over 0.188 in. in diameter or distance between flats, the diameter or distance between flats may be reduced by not more than 0.010 in. without changing the shape of the cross section. Square, hexagonal, or octagonal wire or rod not exceeding 0.188 in. between flats may be turned to a round having a cross-sectional area not smaller than 90 % of the area of the maximum inscribed circle. Fillets, preferably with a radius of 3/8 in., but

APPENDIX B: Detail Drawing Specimen for Tensile Test



Front view
Scale: 2:1



Isometric view
Scale: 1:3

Isometric view
Scale: 1:2

Note Refer ASTM E8-04:

[1]-The reduction section may have a gradual taper from the ends toward the center with the ends not more than 1% larger in diameter than the center (controlling dimension).

[2]-The length of the reduced section may be increased to accommodate an extensometer of any convenient gage length.

[3]-The extensometer gage length for the determination of yield behavior shall not exceed 80 % of the distance between grips.



UNIVERSITI TEKNIKAL MALAYSIA MELAKA

DRAWING TITLE Specimen for tensile test
(Engine Mounting)

SIZE	DESCRIPTION	REV
A4	Project Sarjana Muda (PSM)	0
SCALE	1:1	WEIGHT(kg) XXX
		SHEET 1/1

APPENDIX C: Result of Tensile Strength (SAMPLE 1)

Mild Steel

high strenght steel sample 1



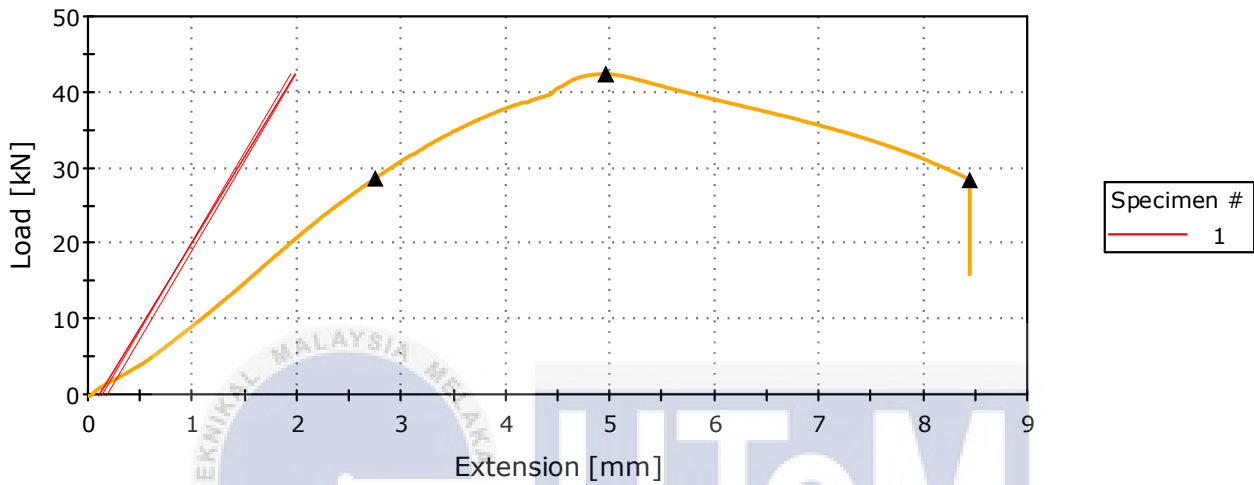
	Maximum Load [kN]	Tensile stress at Maximum Load [MPa]	Load at Tensile strength [kN]	Extension at Break (Standard) [mm]
1	44.15	585.32	44.13	8.21

	Load at Break (Standard) [kN]	Load at Yield (Lower) [kN]	Tensile stress at Yield (Lower) [MPa]	Load at Yield (Zero slope) [kN]
1	31.05	-----	-----	44.15

	Tensile stress at Yield (Zero slope) [MPa]
1	585.32

APPENDIX C: Result of Tensile Strength (SAMPLE 2)

high strenght steel sample 2



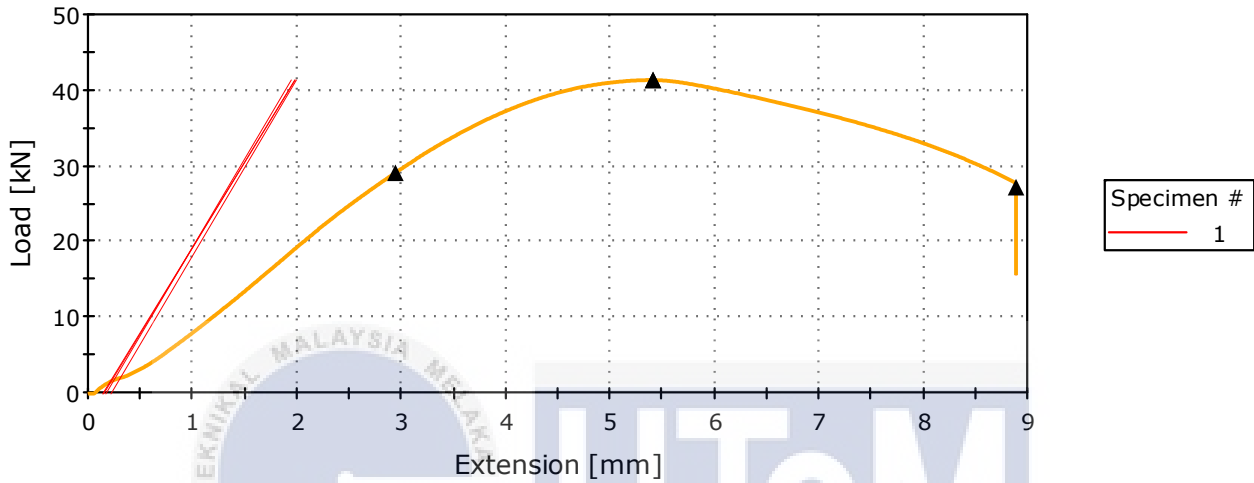
	Maximum Load [kN]	Tensile stress at Maximum Load [MPa]	Load at Tensile strength [kN]	Extension at Break (Standard) [mm]
1	42.36	691.70	42.08	8.44

	Load at Break (Standard) [kN]	Load at Yield (Lower) [kN]	Tensile stress at Yield (Lower) [MPa]	Load at Yield (Zero slope) [kN]
1	28.46	-----	-----	42.36

	Tensile stress at Yield (Zero slope) [MPa]
1	691.70

APPENDIX C: Result of Tensile Strength (SAMPLE 3)

high strenght steel sample 3



	Maximum Load [kN]	Tensile stress at Maximum Load [MPa]	Load at Tensile strength [kN]	Extension at Break (Standard) [mm]
1	41.31	694.91	41.30	8.88

	Load at Break (Standard) [kN]	Load at Yield (Lower) [kN]	Tensile stress at Yield (Lower) [MPa]	Load at Yield (Zero slope) [kN]
1	27.23	-----	-----	41.31

	Tensile stress at Yield (Zero slope) [MPa]
1	694.91

APPENDIX D - Sample Calculation for Tensile Test

Calculation of ultimate tensile strength, yield strength, fracture strength, percent elongation and percent reduction in area:

$$\text{Ultimate Tensile Strength, } \sigma_{ult} = \frac{F_{ult}}{\frac{\pi}{4}(d^2)}$$

$$\sigma_{ult} = \frac{44.15 \times 10^3}{\frac{\pi}{4}(0.0088^2)}$$

$$\sigma_{ult} = 725.9 \text{ MPa}$$

$$\text{Yield Strength, } \sigma_{ys} = \frac{F_{ys}}{\frac{\pi}{4}(d^2)}$$

$$\sigma_{ys} = \frac{32 \times 10^3}{\frac{\pi}{4}(0.0088^2)}$$

$$\sigma_{ys} = 526.13 \text{ MP}$$

$$\text{Fracture Strength, } \sigma_F = \frac{F_F}{\frac{\pi}{4}(d^2)}$$

$$\sigma_{ys} = \frac{31 \times 10^3}{\frac{\pi}{4}(0.0088^2)}$$

$$\sigma_{ys} = 510.51 \text{ MPa}$$

$$\text{Percent Elongation} = \frac{(l_f - l_o)}{l_o} \times 100\%$$

$$\% EL = \frac{55 - 50}{50} \times 100\%$$

$$\% EL = 10 \%$$

$$\text{Percent Reduction in area} = \frac{(A_o - A_f)}{A_o} \times 100\%$$

$$\% RA = \frac{8.8 - 6.4}{8.8} \times 100\%$$

$$\% RA = 27.3 \%$$

APPENDIX E: Hardness Conversion Table

ACCIAI E GHISE STEELS AND CAST IRON

VICKERS HV30	P e r C o i l l i n d r i	R O C K W E L L			R O C K W E L L			R O C K W E L L		
		C	D	A	45 N	30 N	15 N	45 N	30 N	15 N
1710		68	77	85.5	75.5	84.5	93.3			
1663		105	67	76	85	74.5	83	93		
1556		104	66	75.5	84.5	73	83	92.5		
1478		103	65	74.5	84	72	82	92		
1400		101	64	74	83.5	71	81	—		
1323		99	63	73	83	70	80	91.5		
1245										
1160										
1076										
1004										
940										
903										
870										
840										
813										
787										
762		97	62	72.5	82.5	69	79	91		
738		94	61	71.5	81.5	67.5	78.5	90.5		
715		92	60	71	81	66.5	77.5	90		
693		90	59	70	80.5	65.5	76.5	89.5		
672		87	58	69	80	64	75.5	—		
652		84	57	68.5	79.5	63	75	89		
632		81	56	67.5	79	62	74	88.5		
612		79	55	67	78.5	61	73	88		
593		77	54	66	78	59.5	72	87.5		
575		76	53	65.5	77.5	58.5	71	87		
558		74	52	64.5	77	57.5	70.5	86.5		
542		497	72	64	76.5	56	69.5	86		
526		485	70	63	76	55	68.5	85.5		
510		475	69	62	75.5	54	67.5	85		
495		462	68	61.5	74.4	52.5	66.5	84.5		
480		450	67	60.5	74	51.5	66	84		
466		440	65	60	73.5	50	65	83.5		
453		433	64	59	73	49	64	83		
440		423	63	58.5	72.5	48	63	82.5		
428		413	61	57.5	72	46.5	62	82		
416		405	59	57	71.5	45.5	61.5	81.5		
404		395	58	56	71	44.5	60.5	81		
392		387	56	55.5	70.5	43	59.5	80.5		
381		377	55	54.5	70	42	58.5	80		
370		368	54	54	69.5	41	57.5	79.5		
360		359	53	53	69	39.5	56.5	79		
350		350	52	52.5	68.5	38.5	56	78.5		
341		341	51	51.5	68	37	55	78		
332		332	50	50.5	67.5	36	54	77		
323		323	49	50	67	35	53	76.5		
314		314	48	49	66.5	33.5	52	76		
306		306	46	48.5	66	32.5	51.5	75.5		
298		298	45	47.5	65.5	31.5	50.5	75		
290		290	44	47	65	30	49.5	74.5		
283		283	43	46	64.5	29	48.5	74		
276		276	42	45.5	64	28	47.5	73.5		
269		269	41	44.5	63.5	26.5	47	72.5		
262		262	40	44	63	25.5	46	72		
256		256	39	43	62.5	24	45	71.5		
250		250	38	42.5	62	23	44	71		
244		244	—	41.5	61.5	22	43	70.5		
239		239	37	41	61	20.5	42	70		
234		234	36	40	60	19.5	41.5	69.5		
225		216	34	16.5						
210		210	33	15						
205		205	32	14						
200		200	—	12.5						
195		195	31	11						
190		190	—	9.5						
185		185	30	8						
180		180	29	7						
176		176	28	6						
172		172	27	5						
169		169	26	4						
165		165	25	3						
160		160	24	2						
157		157	23	1						
153		153	22	0						
150		150	21	—						
146		146	20	—						
144		144	19	—						
141		141	18	—						
139		139	17	—						

COLORE	SCALA SCALE	APPLICAZIONE FIELD OF APPLI
	HRC	acciai duri, temprati hardened steel of high
	HRD	acciai duri, temprati hardened steel of med
	HRA	acciai duri, temprati sottile, cementazioni superficial hardness, c
	HR45N HR30N HR15N	come HRA e spessori as HRA for thin sheet,
	HRG	acciai di media durezza medio spessore for steel, cooper alloy, for hardness slightly h
	HRK	acciai di media durezza medio spessore for steel, cooper alloy, thickness
	HRB	acciai di media durezza medio spessore for steel, cooper alloy, thickness
	HRE	come HRB per durezza as HRB for hardness lo
	HRF	come HRE as HRE, annealed copp
	HR45T HR30T HR15T	come HRG - B - E - F pe as HRG - B - E - F for th
	HV 30	per tutti i metalli ferrosi zione dello spessore del for hard and soft ferrous test load in connection l and hardness of test sar
	HB 30	per metalli ferrosi non te in funzione dello spessore for soft ferrous metals, u in connection between ttness of test sample
	HV	per metalli non ferrosi sc ne dello spessore del prc for all non ferrous metals load in connection betwe hardness of test sample
	HB 5	alluminio puro, rame, otto pure aluminium, copper, a

METALLI NON FERROSI NO IRON METALS

VICKERS HV	BRINELL HB 5	G	ROCKWELL C	ROCKWELL B
198	195	82	92	91
195	189	81	90	89
191	184	80	88	87
188	179	78	86	85
185	175	77	84	83
182	171	76	82	81
179	167	75	80	79
176	163	74	78	77
173	160	73	76	75
171	157	72	74	73
168	154	71	72	71
165	151	70	70	69
163	148	69	68	67
160	145	68	66	65
157	142	67	64	63
156	140	66	62	61
153	137	65	60	59
151	135	64	58	57
149	133	63	56	55
147	130	62	54	53
145	128	61	52	51
142	126	60	50	49
140	124	59	48	47
138	122	58	46	45



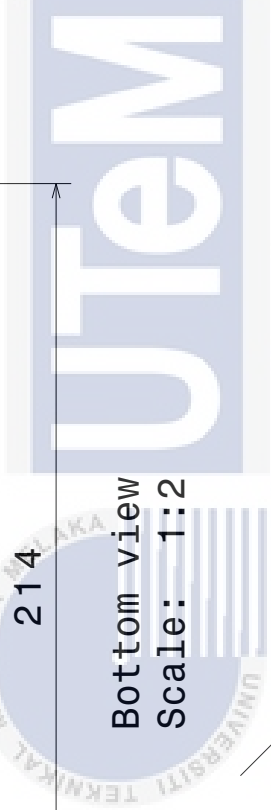
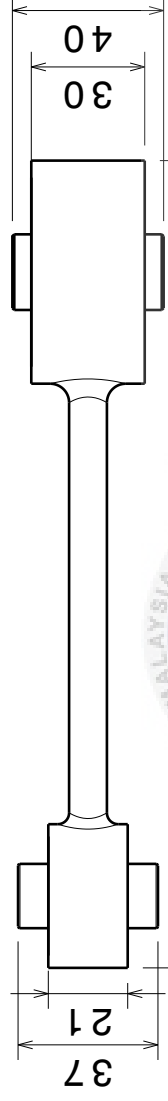
SD



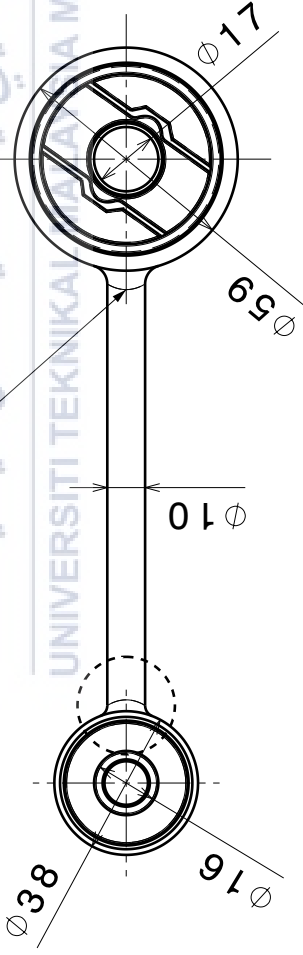
S

4 3 2 1 A

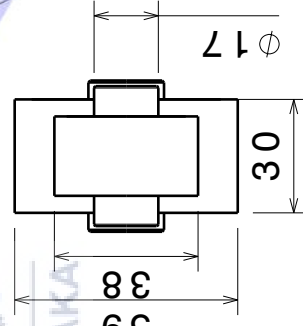
**APPENDIX F: Detail Drawing
Proton SAGA Engine Mounting Component**



Bottom view
Scale: 1:2



Front view
Scale: 1:2



Left view
Scale: 1:2



Isometric view
Scale: 1:2

This drawing is our property. It can't be reproduced or communicated without our written agreement.



UNIVERSITI TEKNIKAL MALAYSIA MELAKA

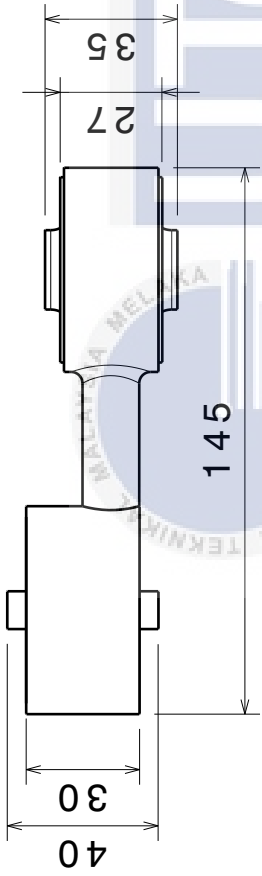
DRAWING TITLE
Engine Mounting Component (Saga)

SIZE	DESCRIPTION	REV
A4	Project Sarjana Muda (PSM)	0
SCALE	WEIGHT (kg)	SHEET
1:1	XXX	1/1

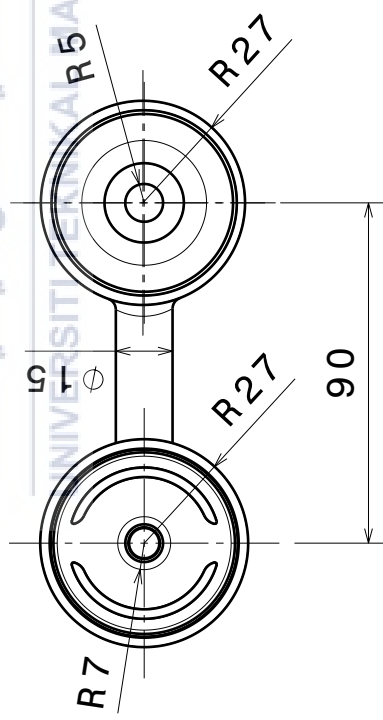
D A

APPENDIX G: Detail Drawing

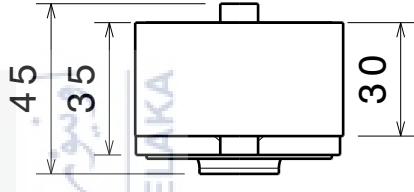
Perodua KANCIL Engine Mounting Component



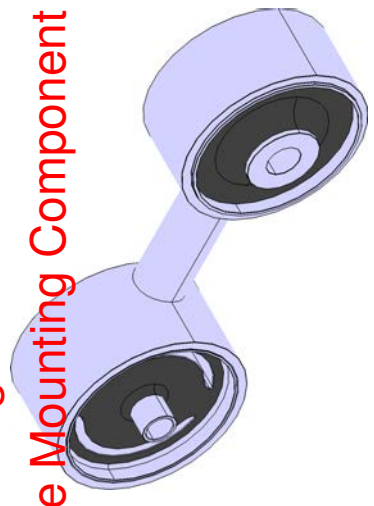
Bottom view
Scale: 1:2



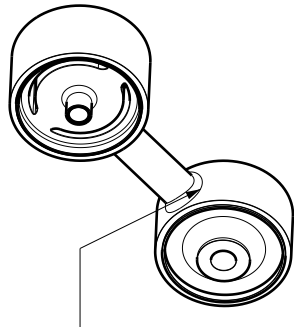
Front view
Scale: 1:2



Left view
Scale: 1:2



Isometric view
Scale: 1:2



Welding Area

This drawing is our property. It can't be reproduced or communicated without our written agreement.



DRAWN BY Azmeirul		DATE 12/8/2016
CHECKED BY XXX		DATE XXX
DESIGNED BY XXX		DATE XXX
DRAWING TITLE Engine Mounting Component (Kancil)		
SIZE A4	DESCRIPTION Project Sarjana Muda (PSM)	REV 0
SCALE 1:1	WEIGHT (kg) XXX	SHEET 1/1

